Quarterly Journal of the Royal Meteorological Society

Mechanisms initiating heavy precipitation over Italy during the HyMeX Special Observation Period 1: A numerical case study using two mesoscale models

Journal:	*QJRMS*
Manuscript ID:	QJ-15-0122.R1
Wiley - Manuscript type:	HyMeX Special Issue
Date Submitted by the Author:	n/a
Complete List of Authors:	Barthlott, Christian; Karlsruhe Institute of Technology (KIT), Institute of Meteorology and Climate Research Davolio, Silvio; ISAC-CNR,
Keywords:	deep convection, high impact weather, COSMO model, MOLOCH model, HyMeX

Mechanisms initiating heavy precipitation over Italy during the HyMeX Special Observation Period 1: A numerical case study using two mesoscale models

Christian Barthlott[a]*and Silvio Davolio[b]

[a]*Institute of Meteorology and Climate Research (IMK-TRO), Karlsruhe Institute of Technology (KIT), Karlsruhe, Germany*

[b]*Institute of Atmospheric Sciences and Climate (CNR-ISAC), Bologna, Italy*

*Correspondence to: C. Barthlott, Institute of Meteorology and Climate Research (IMK-TRO), Karlsruhe Institute of Technology (KIT), Wolfgang-Gaede-Str. 1, 76131 Karlsruhe, Germany.

E-mail: christian.barthlott@kit.edu

This study focuses on the initiation of deep convection during a heavy precipitation episode which occurred during the first Special Observation Period (SOP 1) of the Hydrological cycle in the Mediterranean Experiment (HyMeX). In the course of 14 and 15 October 2012 (Intensive Observation Period 13), intense convective events affected southern France, Corsica, and several regions of Italy. Numerical simulations are performed with two state-of-the-art numerical weather prediction models (i. e. COSMO and MOLOCH) driven by the same initial and boundary data and operated on an identical domain. With this set-up, the sensitivity of the model results to horizontal grid spacing and terrain elevation is assessed. Furthermore, model outputs are compared to observations from rain gauges, radars, and radiosondes, ~~especially available for~~ made during the campaign. Although the higher-resolution runs show a higher correlation to observed precipitation, the influence of model grid spacing on total precipitation amount or timing is rather weak. ~~Furthermore, we find that the total rain amount does not increase with model resolution.~~ Since the overall performance of both mesoscale models is fairly good, they are used together to investigate the physical processes characterising IOP 13. In particular, the differences in the location and timing of convection between the simulations are used to identify and explore the processes that need to be well represented in order to reproduce adequately the mechanisms initiating heavy precipitation in the Mediterranean region.

Key Words: deep convection, high impact weather; COSMO model; MOLOCH model; HyMeX

Prepared using qjrms4.cls

Received ...

1. Introduction

Most of the Mediterranean countries are regularly affected by heavy precipitation events and devastating flash floods during the late summer and autumn. Precipitation amounts of more than 100 mm in less than 6 hours are not uncommon in these regions (Romero *et al.* 2000; Ricard *et al.* 2012; Rebora *et al.* 2013). This high-impact weather is often associated with midlatitude cyclones and embedded deep convection or quasi-stationary mesoscale convective systems with a continuous cell renewal at the same location (e.g., Bech *et al.* 2011; Ducrocq *et al.* 2008; Buzzi *et al.* 2014). Despite the toll that these events take on life and property, quantitative precipitation forecasting (QPF) still remains a challenge for state-of-the-art numerical weather prediction (NWP) models. Although the synoptic scale setting (Rotunno and Houze 2007; Nuissier *et al.* 2008) and the phenomena responsible for triggering convection are broadly known (Jorgensen and Weckwerth 2003; Bennett *et al.* 2006), the forecasting skill for heavy convective showers is still low. A large part of the inaccuracy results from the difficulties ~~to initiate~~ in initiating convection at the right place and time (e.g. Barthlott *et al.* 2011). Besides uncertain initial and boundary conditions, inaccuracies of numerical methods and/or the incomplete description of physical processes influence the performance of NWP models. In particular, the poor representation of boundary-layer processes over complex terrain is supposed to play a major role for QPF deficiencies (e.g. Barthlott *et al.* 2011; Burton *et al.* 2013; Hanley *et al.* 2014).

Improving the understanding and forecasting of the processes leading to heavy rainfall and floods was the main objective of the first field campaign - Special Observation Period - SOP 1 (Ducrocq *et al.* 2014) of the international research project HyMeX (Drobinski *et al.* 2014). While the general objective of HyMeX is to advance the scientific knowledge of water cycle variability in the Mediterranean area, thus studying phenomena distributed on a wide range of spatial/temporal scales (from the single event to ~~the~~ decadal variability), the SOP 1 focused on the specific topic of heavy precipitation. During the two months of monitoring and modelling activities of SOP 1 in autumn 2012, several Intensive Observation Periods (IOPs) were conducted in relation to severe weather events affecting the hydro-meteorological sites in the western Mediterranean target area, in Spain, France, and Italy. During IOPs, monitoring activities were intensified and instrumentation especially deployed for the campaign was activated, such as instrumented aircraft, boundary-layer pressurised balloons, radars and lidars, radiosoundings (both at conventional WMO launch sites and at ad hoc locations). This allowed to ~~collect~~ the collection of a huge amount of observations and to document with unprecedented accuracy a number of precipitating systems over the Mediterranean basin along the whole life cycle, from triggering to the mature phase to dissipation. Several recent studies already used the available observational and modelling database, demonstrating its usefulness for obtaining a better understanding of heavy rainfall in the Mediterranean (Barthlott *et al.* 2014; Ferretti *et al.* 2014; Manzato *et al.* 2015).

Along this line In a similar manner, the present study is devoted to the investigation of the severe weather event which occurred during IOP 13 (14-15 October 2012) and was characterised by intense precipitation progressively affecting southern France, Corsica and Italy from west to east. As described in more detail in Section 3, a cold trough extending over the Mediterranean basin and a frontal system travelling eastwards, together with the outbreak of Mistral, established favourable conditions for the development of convective systems. This event is particularly interesting, because several precipitating (mainly convective) systems developed and organised in different areas. Hence, one objective of this study is to identify and describe the mechanisms leading to convection initiation and to assess whether the forcing is on the large scale or on the mesoscale (or a combination of both). In this respect, it also seems to be particularly interesting to analyse the role of mountainous islands: being located upstream of the main precipitation region over Italy, Corsica and Sardinia may modify the westerly/southwesterly flow, which provides moisture in the lower layers, but may also directly trigger convection (Barthlott and Kirshbaum 2013). To reach this objective, two state-of-the-art NWP models driven by the same initial and boundary global data are employed implementing two horizontal grid-spacing configurations each. Instead of performing a solely quantitative model intercomparison, the

two models COSMO and MOLOCH (described in Section 2) are employed in a synergistic way in order to address some technical and physical aspects related to the simulation and investigation of IOP 13. Moreover, model results are exploited together with the available observations to gain insights into the relevant processes responsible for the heavy rainfall event, which need to be accurately simulated and to detect possible model deficiencies. In particular, the role of the orography is analysed extensively. The analysis does not focus solely on rainfall, but also on other relevant meteorological fields as well as on vertical thermodynamic profiles.

2. Numerical models

2.1. *The COSMO model*

The COnsortium for Small-scale MOdeling (COSMO) model is a non-hydrostatic regional weather forecast model (Schättler *et al.* 2013) used for operational weather forecasting by the Deutscher Wetterdienst (DWD, German Weather Service) and several other European weather services. It employs an Arakawa C-grid for horizontal differencing on a rotated latitude/longitude grid. To minimise problems resulting from the convergence of the meridians, the pole of the grid is rotated such that the equator runs through the centre of the model domain. In the vertical, a terrain-following, hybrid height coordinate with 50 levels is used. The lowest level is at a height of 10 m, and 12 of them are in the lowest 1000 m. The vertical distance increases to about 1 km near the upper boundary (21.5 km). We used a two-time level Runge-Kutta method (Wicker and Skamarock 2002) for time integration. A multi-layer soil vegetation model (TERRA-ML, Doms *et al.* 2011) including soil moisture is implemented. The microphysics scheme includes riming processes (graupel formation) and predicts cloud water, rain water, cloud ice, snow, and graupel. Baldauf *et al.* (2011) stated that a more sophisticated two-moment scheme shows only minor differences in most cases. To investigate grid spacing effects on the forecast of convective precipitation, numerical runs were performed with grid spacings of 2.8 km (522×432 grid points) and 1 km (1446×1199 grid points). This enables the parameterisation of deep convection to be switched off. However, shallow convection is still parameterised using a modified Tiedtke scheme (Tiedtke 1989). We used model version 5.0.

Table 1. Model names.

model	Δx (km)	name
COSMO	2.8	C2
COSMO	1	C1
MOLOCH	2.3	M2
MOLOCH	1.5	M1

2.2. *MOLOCH*

MOLOCH is a non-hydrostatic, fully compressible, convection-permitting model (Buzzi *et al.* 2014) developed by the Institute of Atmospheric Sciences and Climate (CNR ISAC). It employs a hybrid terrain-following vertical coordinate, depending on air density and relaxing smoothly to horizontal surfaces away from the Earth's surface. Time integration is based on an implicit scheme for the vertical propagation of sound waves, while explicit, time-split schemes are implemented for integration of the remaining terms of the equations of motion. Three-dimensional advection is computed using the Eulerian weighted average flux scheme (Billet and Toro 1997). The atmospheric radiation is computed with a combined application of the Ritter and Geleyn (1992) scheme and the ECMWF scheme, employing 14 channels for the IR and VIS bands (Morcrette *et al.* 2008). The turbulence scheme is based on an E-l order 1.5 closure theory, where the turbulent kinetic energy equation (including advection) is evaluated. The soil model (which includes soil moisture) uses seven layers whose depths increase moving downward, and takes into account the observed geographical distribution of different soil types and soil physical parameters. The recently upgraded microphysical scheme was initially based on the parameterisation proposed by Drofa and Malguzzi (2004). The spectral properties of clouds are taken into account by assuming a generalised gamma distribution function, while the size of hydrometeors (rain, snow, and graupel) is assumed to be exponentially distributed. In the present study, MOLOCH is implemented with 50 vertical levels and two horizontal grid spacings of 2.3 km (658×562 grid points) and 1.5 km (962×834 grid points) on the same geographical domain than as COSMO.

2.3. *Setup of numerical experiments*

The abbreviations of the COSMO and MOLOCH configurations used in this paper are given in Table 1. For this study, we used the same initial and boundary data for both models, i. e. 6-hourly global analyses of the European Centre for Medium-Range Weather Forecast (IFS-ECMWF) with a horizontal resolution of 0.2° (approx. 22 km). In order to bridge the gap with the global model fields and to provide hourly boundary conditions for our high-resolution models, a run with intermediate resolution (around 8 km) was conducted over an integration domain including western and central Europe as well as part of the Atlantic area. In more detail, C2 and C1 are both nested in a COSMO run with 7 km grid spacing with deep convection being parameterised while M2 and M1 are both nested into the BOLAM hydrostatic model with 8 km horizontal grid spacing. (Buzzi *et al.* 2014). It is worth noting that the high-resolution integration is not started at the same instant of the parent model analysis in order to prevent an effective sudden drop of grid resolution from the global data to the high-resolution grid based on pure interpolation. Instead, using a 1-h forecast as initial condition allows for a dynamic downscaling with a suitable ratio of grid resolutions. The domains of both COSMO and MOLOCH simulations, together with the COSMO model orography at 2.8 km and 1 km horizontal resolution, are shown in Figure 1. The MOLOCH model orography is very similar to those of the COSMO model (not shown). Moreover, both model orography data sets are similarly smooth, as the spatial standard deviation (C2.8: 465 m; C1: 476 m; M2: 471 m, M1: 472 m) is almost identical in all configurations and their probability distributions are almost congruent (not shown). Both models use external data based on 30-arc-second (1-km) Global Land Base Elevation Project (GLOBE) orography, the Global Land Cover 2000 Project (GLC 2000) for a harmonized land cover, and the Food and Agriculture Organization of the United Nations (FAO) Digital Soil Map of the World (DSMW). Minor differences may occur due to different procedures used in the pre-processing to interpolate the data on the respective model grids.

In this study, we will investigate convective activity in several sub domains: Liguria (LG), Northeastern Italy (NEI), Tuscany

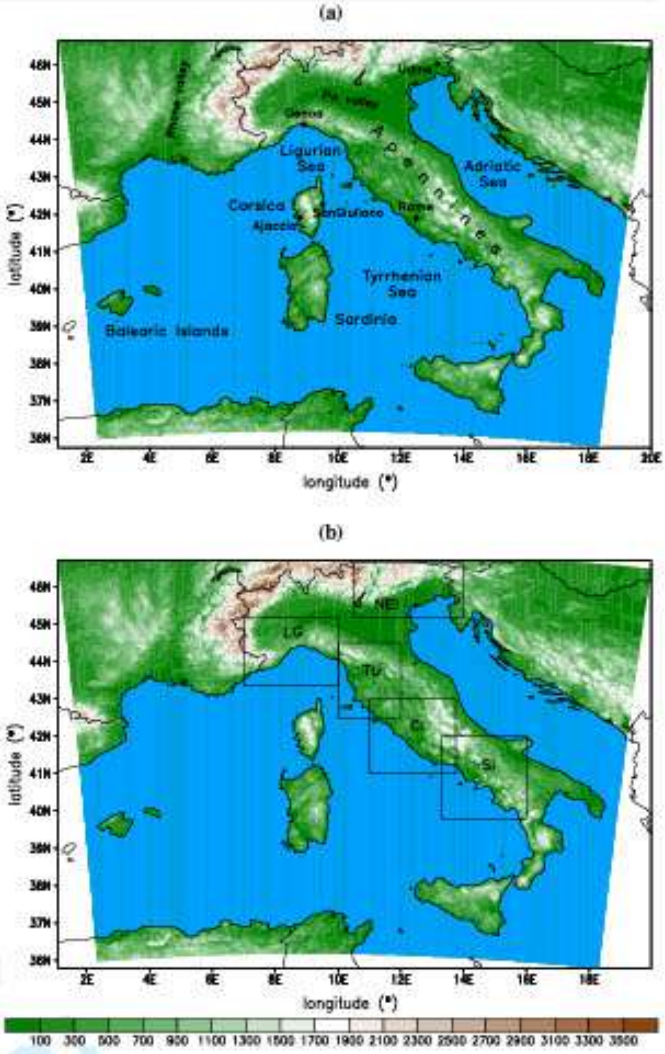

Figure 1. COSMO and MOLOCH simulation domain with COSMO model orography at 2.8 km (a) and at 1 km horizontal grid spacing (b) in m amsl. The black rectangles in (b) indicate the areas for spatial integration of precipitation (TU: Tuscany, NEI: North East Italy, LG: Liguria, CI: Central Italy, SI: South Italy).

(TU), Central Italy (CI), and Southern Italy (SI). These sub domains are depicted as rectangles in Figure 1b. In order to cover the entire event and also to evaluate the sensitivity of model predictions on the initialisation time and forecast range, two sets of simulations are implemented. The runs with intermediate resolution driven by ECMWF global analyses are initialised at 1200 UTC, 14 October and at 0000 UTC, 15 October, respectively. Both simulations end at 0000 UTC on 16 October. The high-resolution simulations (COSMO 2.8 and 1 km; MOLOCH 2.3 and 1.5 km) are initialised at 1300 UTC on 14 October and 0100 UTC on 15 October, respectively. Output is provided every 30 min. At first, we will focus on the results obtained from the runs initialised at 1300 UTC on 14 October, but we will also evaluate the runs started at the later time in the case of interesting features occurring late in the 35-h simulation period.

3. HyMeX Intensive Observation Period 13

3.1. Synoptic situation

During the first field campaign (SOP 1) of the HyMeX project, an Intensive Observation Period was performed between 14 and 15 October 2012 (IOP 13) as a consequence of foreseen ~~intense frontal precipitation first over~~ predicted intense frontal precipitation initially over the coastal areas of France and later over northern and central Italy. The synoptic situation on 14 October (Figure 2) was slowly evolving and dominated by a cold upper level trough extending from the British Islands Isles over France, towards northern Spain. While moving eastwards over the Mediterranean basin, the trough progressively deepened in the course of the day. Associated with the trough, a cold front entered the Mediterranean in the night between 14 and 15 October and swept rapidly from France to Italy during the following day. Moreover, in the early morning of 15 October, a shallow pressure minimum developed over the Gulf of Genoa, associated with a potential vorticity (PV) anomaly aloft. In the evening, the cut-off process completed over Northern Italy and the low moved eastwards over the Adriatic Sea, pushing the associated precipitation over the Balkan area by the early morning of 16 October.

3.2. Mesoscale features and observations

On the mesoscale, this episode was characterised by the intrusion of Atlantic cold air into the warmer Mediterranean area, which favoured atmospheric instability and induced low-level warm and moist air advection ahead of the front towards Corsica and the Italian coast. As described in Ferretti *et al.* (2014), the main convective activity was initially located in the warm sector ahead of the front (Figures 3a, b), while it later was directly triggered by the narrow cold frontal system (Figures 3c, d). Weak rainfall was already observed in the morning of 14 October over western Italy and southeastern France and intense pre-frontal precipitation affected Liguria in the afternoon (50-75 mm between 1800 and 0000 UTC, Figure 4b), when several convective systems were triggered along a line over the Gulf of Genoa (Figure 3a). This line organised in correspondence to an intense low-level southwesterly jet north of Corsica, impinging on the northern Apennines and the Maritime Alps. This jet was monitored by a boundary-layer pressurised balloon launched in the morning of 14 October (0621 UTC) from Minorca Island, which indeed registered a remarkable increase of wind speed, reaching 20 m s^{-1} while approaching the Ligurian coast. Later in the early morning of 15 October (Figure 3b), rainfall moved also over Tuscany and ~~reinforced~~ intensified over Liguria, where high lightning frequency indicated deep convective activity. In the following hours, the Mistral abruptly entered the western Mediterranean basin from the Rhône valley and the front progressed eastwards. The LEANDRE 2 water vapour lidar (Bruneau *et al.* 2001; Flamant 2013) flying onboard the research aircraft ATR42 operated by SAFIRE monitored the moist planetary boundary layer (PBL) (mixing ratio up to 12 g kg^{-1}) in flight AS49 on 15 October 2012 (0747-1059 UTC) within the low-level flow over the central Tyrrhenian Sea, east of Sardinia (not shown). Here, the wind turned to southerly directions and low-level convergence developed in front of Tuscany's coast. Convective systems were triggered close to the Elba Island for several hours (Figure 3c), starting around 1200 UTC, and also affected internal areas of Tuscany, progressively moving southeastwards. In the meanwhile, colder and drier air associated with the Mistral reached the western coast of Corsica as confirmed by much lower mixing ratios in the PBL (less than 8 g kg^{-1}) measured by the ATR42 (flight AS50 on 15 October 2012, 1225-1349 UTC) at around 1300 UTC on its way back from Bastia to France. Finally, in the afternoon of 15 October, the advancing intense PV anomaly, together with the convergence between southerly warm air and westerly colder air was responsible for the development of several mesoscale convective systems (MCS) in the central and southern Tyrrhenian Sea (Figures 2d, e, f). In the following hours, the associated frontal system moved rapidly towards the Italian peninsula and deep convection reached the Tyrrhenian coast, east of Rome (Figure 3d). A convective line swept over Rome's urban area in the evening, associated with short-lasting but heavy rainfall, while in the night also southern Italy was affected by intense convective precipitation.

Many observing platforms were activated during this IOP, thus allowing for a detailed monitoring of the event. The dense rain gauge network and the Italian radar composite, together with

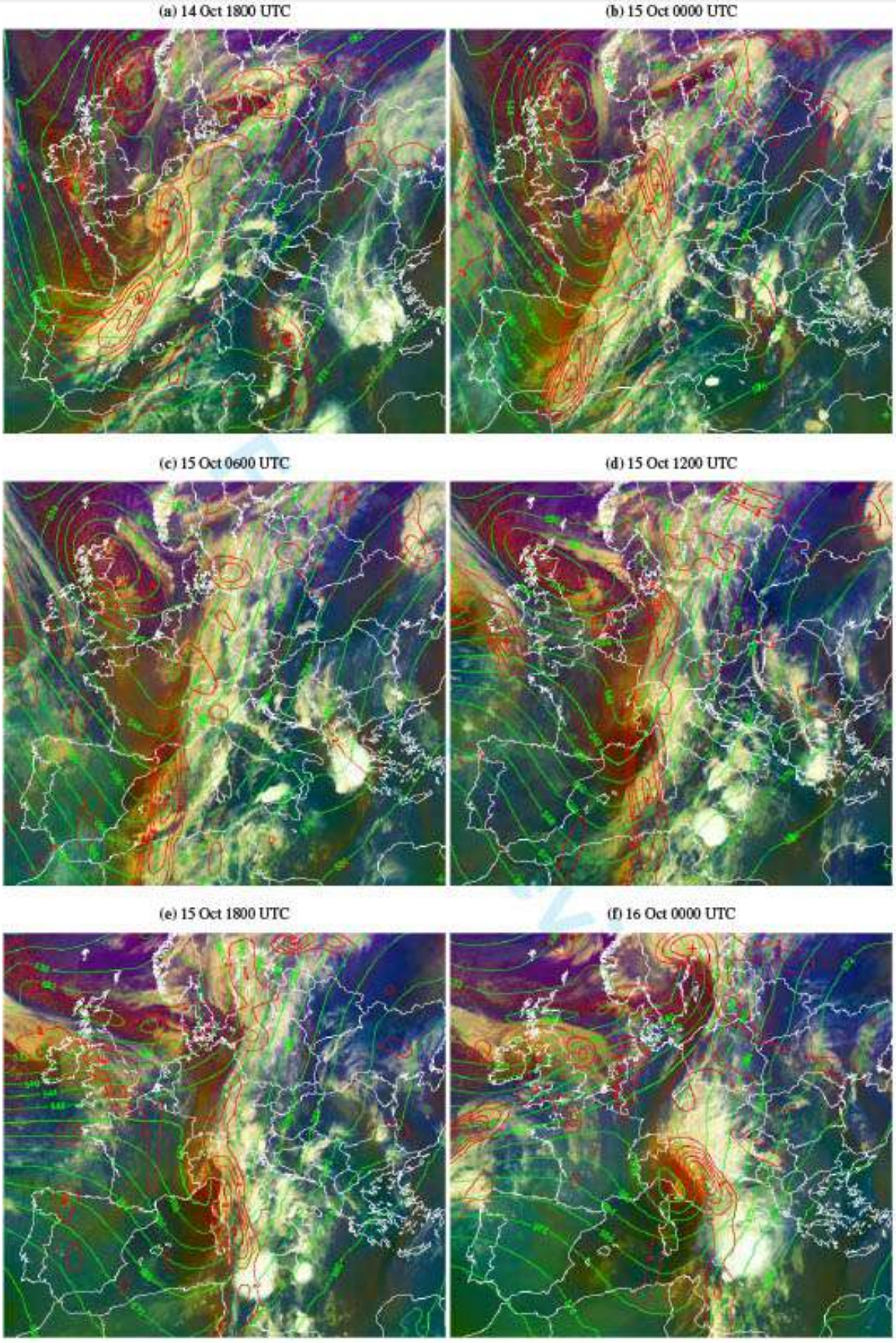

Figure 2. Synoptic analysis over the western Mediterranean region: European Centre for Medium-Range Weather Forecasts (ECMWF) 500 hPa geopotential height (green lines) and positive vorticity advection at 300 hPa (red lines) superimposed to the Meteosat Second Generation SEVIRI AirMass RGB composite EumetSat product. Source: http://www.eumetrain.org

research radar in Rome (Polar 55C managed by CNR ISAC) and in San Giuliano (Corsica, managed by KIT), provided a detailed description of rainfall evolution. Lightning maps (see Figure 11 in Ferretti *et al.*, 2014) indicated the morning (over the Ligurian Sea) and the afternoon (over the central Tyrrhenian Sea) as the two periods characterised by intense convective activity. In more

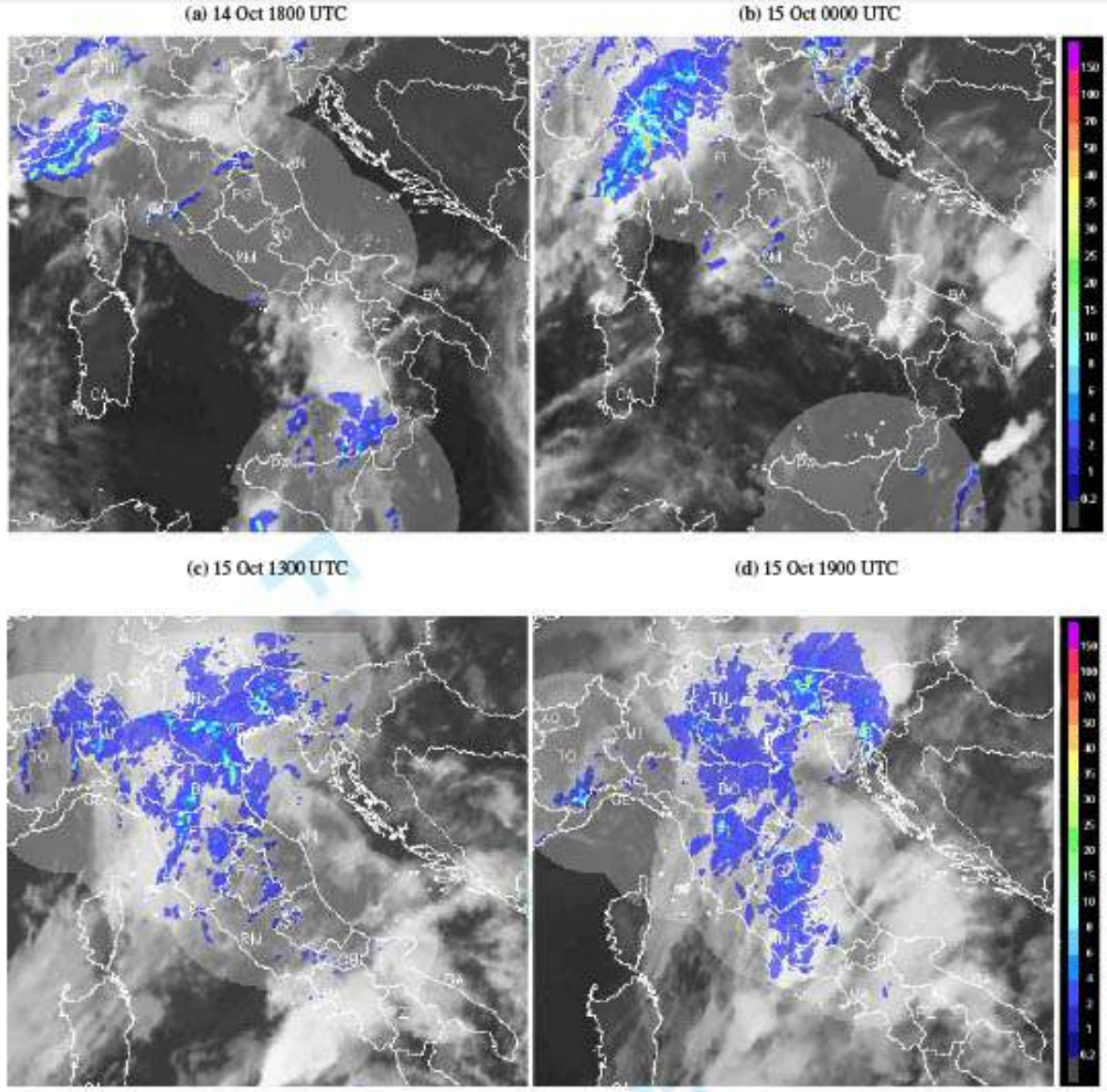

Figure 3. Italian radar composite (rain rate in mm h^{-1}) and IR meteosat image. Courtesy of Italian National Department of Civil Protection (DPC).

detail, 50 mm $(6\ h)^{-1}$ affected a wide area around the city of Genoa (see location in Figure 1a) in the evening of 14 October, reaching 75 mm $(6\ h)^{-1}$ locally over the Ligurian Apennines (Figure 4). Precipitation persisted over the same area in the early morning of 15 October, but also progressively affected Tuscany, where up to 120 mm $(24\ h)^{-1}$ were cumulated in the mountainous areas. However, as shown by radar images (Figure 3), the most intense precipitating systems during the night were located over the sea and organised along a line in the western part of the Genoa gulf, which remained almost stationary for several hours before progressing eastwards and then dissipating close to the Tuscany coast in the early morning.

Over central Italy, the cumulated rainfall was not exceptional (up to 60 mm $(24\ h)^{-1}$), but it is worth noting that at many stations, about 50 mm fell in only two hours and disdrometers recorded a maximum rain rate of 114 mm h^{-1} in correspondence with the passage of the convective line in the evening, at around 1800 UTC.

4. Results

4.1. *Accumulated precipitation*

At first, we analyse the 35-h accumulated precipitation (Figure 5) to obtain a broad overview of the location and amount of precipitation simulated by COSMO and MOLOCH compared to surface observations. With the exception of north-eastern Italy, the main precipitation zones are located near the coast and the mountainous regions of the Apennines. There is considerably less precipitation in the eastern part of Italy towards the Adriatic coast, which is in the lee of the orography with respect to the impinging moist flow.

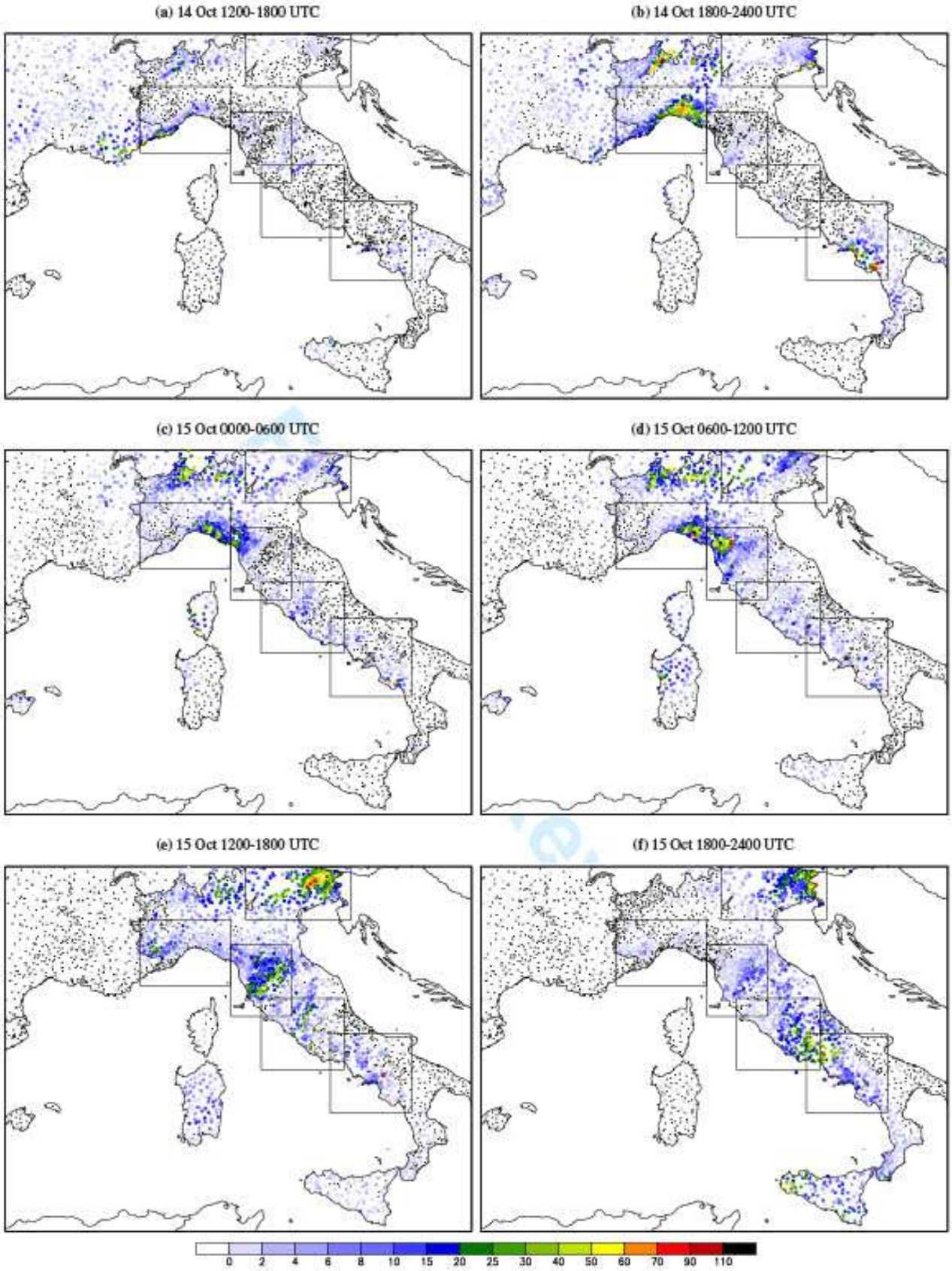

Figure 4. 6-h accumulated precipitation in mm as measured by rain gauges. Black dots indicate rain gauge stations without measured precipitation.

In the Ligurian region, all models simulate an elongated area of precipitation along the coastline from south~~western~~eastern France towards the Po valley. The location of this precipitation area is in good agreement with rain gauge observations. However, observed precipitation amounts (40-80 mm) are considerably weaker than the simulated ones (160-270 mm). It is worth noting that this error is attributed more to a misplaced precipitation line than to an actual overestimation in the simulations. Indeed, models predict

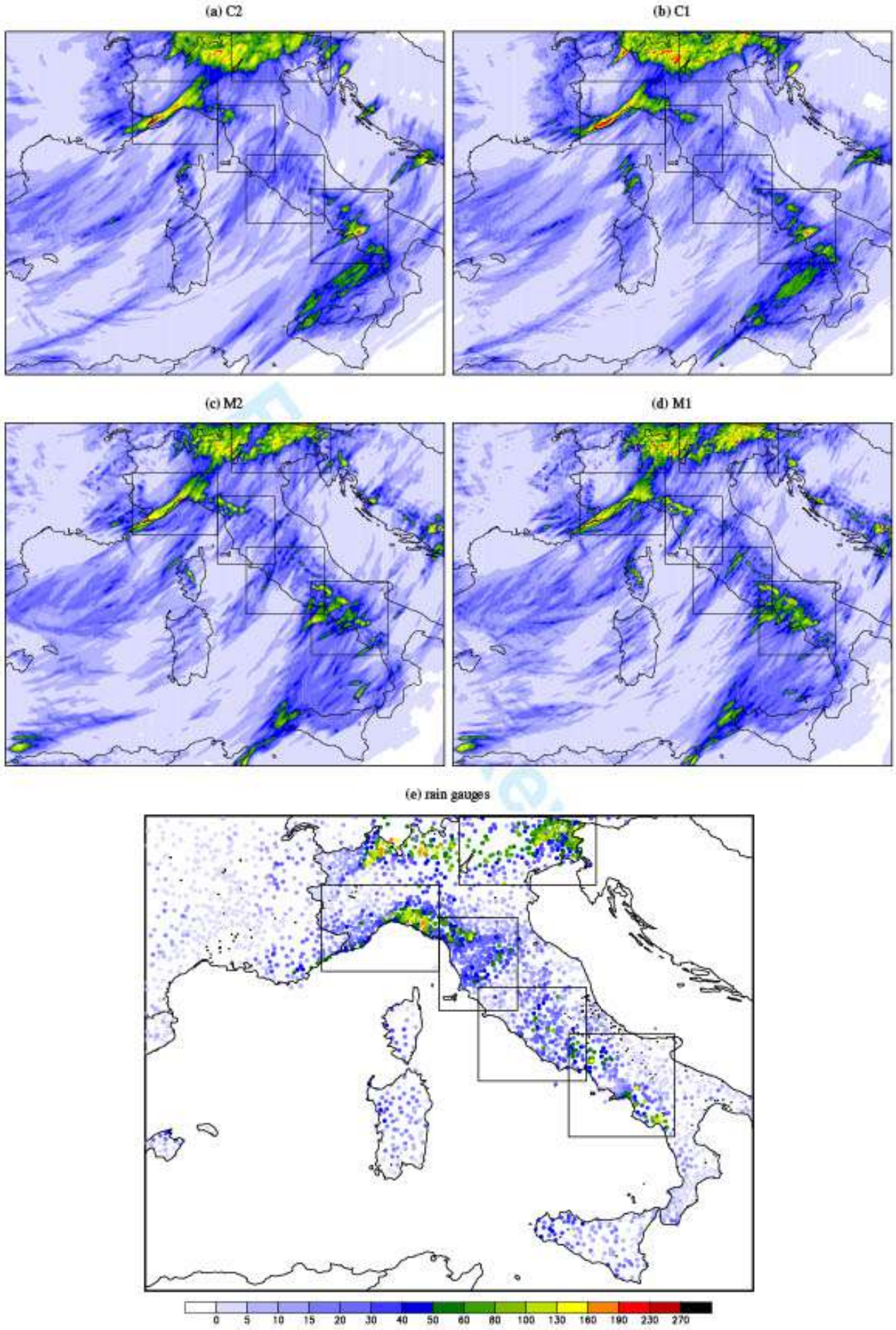

Figure 5. 35-h accumulated precipitation (14 Oct 1300 UTC-16 Oct 0000 UTC) in mm as simulated with COSMO (a)-(b), with MOLOCH (c)-(d), and as observed by rain gauges (e). The black rectangles indicate the boxes already introduced described in Figure 1.

this convective line over the coast, while radar images (Figure 3a) show heavy rainfall (rain rate larger than 100 mm h^{-1}) over the sea, about 20-30 km offshore. In particular, the simulations with the COSMO model provide very large amounts of precipitation (C2 > 270 mm; C1: 230-270 mm). Whereas the region with maximum precipitation is located over or very close to the coastline in the runs C1, M1, and M2, this region is located somewhat north of the coast line in the C2 run. The observed precipitation maximum in the region of Liguria is located further east in the Gulf of Genoa (Figure 5e) with values between 140-160 mm. In that area, the COSMO runs simulate 120-140 mm, whereas both MOLOCH runs simulate maxima of up to 180 mm, but slightly displaced toward northwest.

Concerning the location of precipitation in northern Italy, COSMO and MOLOCH agree reasonably well. The rain gauge measurements show local maxima over the western and eastern Alps (140-180 mm). The numerical simulations, however, reveal higher values of up to 270 mm.

Over Tuscany, observed average rainfall is between 5 and 30 mm with isolated local maxima between 140 and 160 mm over the northern Apennines. Again, both models succeed in reproducing the location of maximum rain amount. The COSMO runs show maximum values between 80 and 120 mm, whereas M2 simulates up to 180 mm and M1 a maximum ranging between 230 and 270 mm.

Rain gauge measurements reveal a maximum between 80 and 100 mm in Central Italy. Both COSMO runs show only moderate values of maximum precipitation (40-60 mm), whereas the MOLOCH runs simulate higher values (M2: 120-140 mm, M1: 160-180 mm). However, the M1 simulation clearly produces the precipitation line oriented in NE-SW direction, which affected the area of Rome (see Figure 1a) in the evening of 15 October. More localised maxima were measured in southern Italy. There is one main convective cell in the centre of this area near the coastline and two smaller ones (to the north-west and to the south-east) in the COSMO simulations. The MOLOCH simulations reveal a number of small-scale convective cells, one of them being located over the sea.

An important finding is the fact that the simulation results do not change substantially with model resolution. Although more small-scale convective cells with somewhat increased intensity are simulated by C1 and M1, the overall structure of convective precipitation remains similar to that predicted by the respective coarser model run. However, the analysis of the total precipitation amount computed for the different boxes (shown in Figure 5) shows a maximum increase (decrease) in precipitation of 25% (-9%) in the simulations (Table 2). In addition, the precipitation amount in the different boxes is not correlated with model resolution, as the C1 and M1 runs do not necessarily simulate higher values than C2 and M2. For ~~a larger HyMeX~~the total simulation domain (HDSD ~~, i.e. the simulation domain~~) (somewhat smaller to avoid edge effects) displayed in Figure 5, however, the accumulated precipitation of both models increases slightly with grid resolution ~~no matter~~ irrespective of whether only the land points or the whole area are considered. It is also interesting to find out whether one model systematically yields more precipitation than the other one. For the ~~larger HyMeX~~ the total simulation domain, M2 and M1 simulate more precipitation than C2 and C1, but when analysing the smaller boxes, it is no longer possible to find a systematic behaviour.

Table 2. 35-h accumulated precipitation for the different boxes in 10^9 ltr (only land points). ~~HD~~ SD denotes the ~~HyMeX~~ simulation domain ~~(i.e. the simulation domain)~~ (somewhat smaller to avoid edge effects) displayed in Figure 5. Numbers in brackets give percentage deviation of C1 (M1) from C2 (M2), respectively. $HDSD_{tot}$ represents the total rain amount (land and sea points).

	C2	C1	M2	M1
LG	1217	1196 (-1.7%)	1174	1087 (-7.4%)
NEI	2013	2089 (+3.8%)	1853	1931 (+4.2%)
TU	493	617 (+25%)	594	554 (-6.7%)
CI	544	497 (-8.6%)	680	766 (+12.6%)
SI	998	991 (-0.007%)	1129	1244 (+10.2%)
~~HD~~SD	10883	11097 (+2.0%)	10999	11212 (+1.9%)
$HDSD_{tot}$	18193	18423 (+1.3%)	18604	18973 (+2.0%)

Although it is not the objective of this study to rank the participating models, we want to compare the simulations with the observed precipitation in a more quantitative way. For this purpose, some statistical error variables for the 35-h accumulated precipitation are listed in Table 3. For these calculations, the model grid points at the respective location of the rain gauges were selected. It can be seen that the root mean square error (RMSE) of the MOLOCH runs are slightly smaller than those of COSMO. While increasing resolution reduces the RMSE of the COSMO model, the RMSE of MOLOCH increases. However, both models

Table 3. Root mean square error ($RMSE$), correlation coefficient (r), and standard deviation (σ) of measured and simulated 35-h accumulated precipitation.

	$RMSE$ (mm)	r	σ (mm)
C2	28.5	0.48	29.5
C1	26.5	0.57	30.1
M2	25.3	0.56	27.6
M1	26.1	0.59	30.4
obs	-na-	-na-	25.8

reveal a higher correlation with the observations in the high-resolution simulations compared to their coarser configurations. The smaller jump in resolution from 2.3 km to 1.5 km in the MOLOCH runs increases the correlation only slightly from 0.56 to 0.59. The COSMO model has a larger jump in resolution (from 2.8 km to 1 km), which seems to be reflected by the stronger correlation increase from 0.48 to 0.57. The standard deviations of the simulations (27.6 mm-30.4 mm) are higher than the observed one, with the M2 run being closest to the measurements.

Finally, in order to assess the sensitivity to the initialisation time of the models, the rainfall accumulated during 15 October, as simulated by the two different sets of experiments (as described in Section 2.3), is compared (not shown). Differences in the total precipitation are not particularly relevant, especially as far as the COSMO runs are concerned. Rainfall prediction over the Alps is slightly improved by the simulations initialised later, since the west-to-east gradient of the observed precipitation fields is reproduced better. The only pronounced difference occurs in the MOLOCH runs initialised at 0100 UTC, 15 October, where the passage of the front in the evening over Tuscany and Central Italy seems to be slightly faster and does not produce the intense convective lines affecting the urban area of Rome. Rainfall is forecast further north, but with the correct timing. These results indicate that the relatively long lead time of the forecasts initialised at 1300 UTC, 14 October, does not represent a limiting factor for our analysis, since those simulations appear to be accurate and close enough to the simulations initialised later. The comments given below will therefore concentrate on the results obtained by the chain simulations initialised on 14 October, since they also cover the first part of the heavy precipitation event affecting Liguria during the evening and the night of 14 October.

4.2. *Temporal evolution of spatially integrated rainfall*

The analysis of the evolution of domain-averaged precipitation computed for the selected boxes (Figure 6) allows ~~to identify~~ the identification of different phases of the event, which are characterised by different mechanisms responsible for convection triggering. Although the rain gauge data are point measurements, the large density of surface observations (see Figure 5e) certainly reduces errors when comparing them to model output available on a continuous grid. Moreover, the analysis of domain-averaged mean values instead of accumulated precipitation is assumed to be less subject to errors than interpolating rain gauge data on the model grid, which can introduce large errors (in particular for convective precipitation).

In the LG region (Figure 6a), the first peak of convective precipitation between 1900-2300 UTC on 14 October is well captured by both models. There are only minor differences between the coarser and finer grid spacing simulations of each model. The peak in the morning of 15 October at 0800 UTC is not simulated adequately: both models simulate their maxima 1-2 h later and with slightly reduced intensity than in the observations. The next local maximum is simulated between 1300-1600 UTC, which is earlier than observed (1700 UTC).

The simulations for NEI (Figure 6b) reveal similar mean precipitation rates for COSMO and MOLOCH throughout almost the entire integration period. Only in the first hours, till 0000 UTC on 15 October, do M1 and M2 predict slightly higher precipitation rates than C1 and C2, whereas after 1400 UTC, it is the other way around. The rain gauge measurements show values similar to the simulations until 0900 UTC on 15 October. The following large increase of the mean precipitation rate up to 6 mm h^{-1} is not captured by the models. However, the analysis of the corresponding 6-h accumulated precipitation maps (Figure 4) reveals that both models correctly simulate intense rainfall over this area. Probably, this relevant underestimation is due to the low density of observations in a large portion of the NEI domain (Figure 4e), where precipitation was quite weak, thus resulting in apparently very high values of observed precipitation.

In TU (Figure 6c), there are two observed precipitation maxima on 15 October, one between 0100-0500 UTC with a maximum

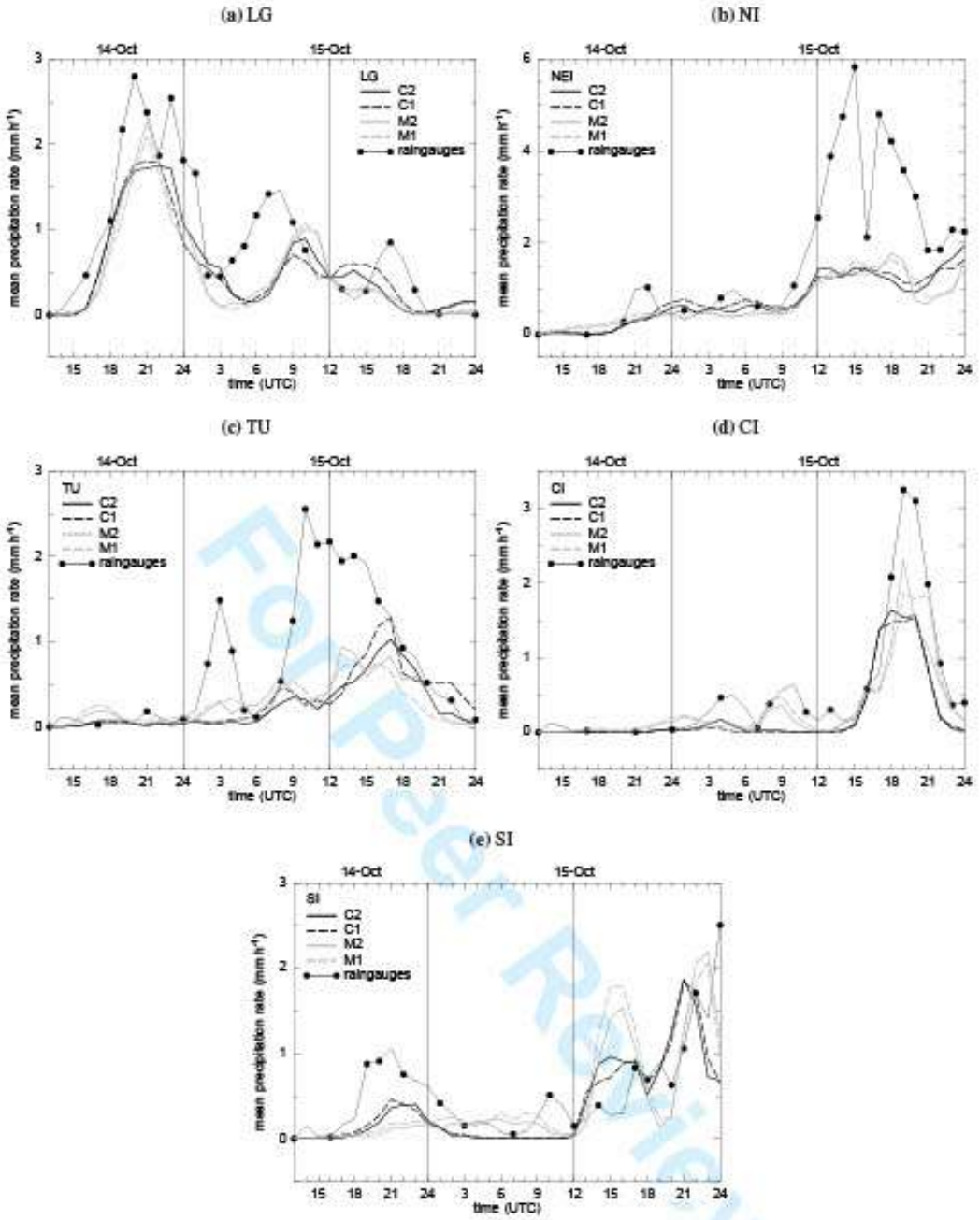

Figure 6. Spatially averaged precipitation for the boxes depicted in Figure 1 (C2: COSMO 2.8 km; C1: COSMO 1 km; M2: MOLOCH 2.3 km; M1: MOLOCH 1.5 km).

mean precipitation of around 1.5 mm h^{-1} and a longer-lasting and more intense event between 0800-2100 UTC with a maximum exceeding 2.5 mm h^{-1}. Irrespective of the configuration, both COSMO and MOLOCH resolve the first episode only vaguely, while the second one is simulated between 1200-1800 UTC (M2 and M1) and between 1300-1900 UTC (C2, C1).

A much better result is achieved for the region of CI (Figure 6d), where the observed rainfall maximum in the evening of 15 October is very well captured by both models, although the simulated mean rain intensity is slightly weaker than observed. There are also two secondary maxima in the rain gauge measurements in the morning of 15 October. These are missed by the COSMO runs, while MOLOCH simulates only the second one with a good agreement in terms of intensity and timing. Thus, it is possible to further investigate the reasons why the COSMO runs do not simulate any rain in that area. An analysis of the low-level wind fields (not shown) displays a southwesterly flow over the Tyrrhenian sea, which is almost perpendicular to the Italian coast of CI. While in the COSMO runs, the winds are deflected towards the north by the presence of the Apennines orography, the MOLOCH runs show more or less undisturbed southwesterly winds over the main mountain ridge. The associated lifting, together with slightly warmer low-level equivalent potential temperatures, leads to convection initiation

in the MOLOCH simulations. The different behaviour of the flow in the two models can be explained by an analysis of the Froude number: assuming a terrain height of 1500 m, the Froude number on the western coast of CI in the C2 run is around 0.4. In the M2 run, however, higher values of around 0.7 are simulated, indicating that the air can more easily flow over the mountains than in the COSMO realisation. Apparently, the correct simulation of thermal stratification is of particular importance and small differences can lead to different flow regimes, which in turn modulate the development of convection.

In SI (Figure 6e), there is an observed peak of precipitation at 2100 UTC on 14 October and after 0900 UTC on the next day, the precipitation increases unsteadily, reaching its maximum value at 0000 UTC on 16 October. The COSMO model captures the first maximum with reduced intensity, whereas both MOLOCH runs simulate only a slight increase of the mean precipitation until 0900 UTC on the next day. In the afternoon of 15 October, both models simulate a rain maximum between 1500 and 1600 UTC, which is overestimated for M2/M1 and rather close to observations for C2/C1. Afterwards, both models simulate an increase of mean precipitation of a magnitude similar to that of the observed one.

To sum up the results concerning the temporal evolution of convective precipitation in the different selected areas, it can be stated that only few of the observed precipitation events are missed by the NWP models and that the simulated mean rain intensity is often weaker than the observed one. The timing of convective precipitation in the model simulations is not sensitive to the model resolution, which seems to influence precipitation intensity only. Almost all of the strongest rain events are captured by COSMO and MOLOCH, but there are cases of moderate intensity, where just one of the models is able to capture the event (e.g. CI: 15 October 1000 UTC or SI: 14 October 2100 UTC). This made us investigate and possibly identify which processes are simulated correctly and which processes are missing in the model simulations.

4.3. *Convection-initiating mechanisms*

The evolution of averaged precipitation displayed in Figure 6 clearly shows the progressive eastward movement of the frontal system and of the associated weather phenomena. The vertically integrated water vapour (IWV, Figure 7b) averaged over the selected boxes also shows an increase in accordance with the initiation of the rainfall events in each area. The maximum values of IWV occur roughly 1-2 h before the respective precipitation maximum. From the analysis of other variables averaged over the same boxes (Figure 7) and of meteorological fields, such as 10-m wind, rainfall, and equivalent potential temperature θ_e (Figure 8), it is also possible to identify three different phases of the IOP 13 event, which are characterised by different mechanisms responsible for triggering the precipitating systems.

During the evening of 14 October, the outbreak of Mistral over the western Mediterranean Sea produced a sharp convergence line in the lower levels of the atmosphere, propagating south-eastwards towards Corsica and Sardinia (Figure 8). Along the northernmost part of this line, ahead of the frontal system, the convergence of warm and moist southerly flow (high θ_e values over LG box as shown in Figure 7a) with colder and drier air, together with the interaction with coastal orography (between France and Italy), produced intense precipitation. The organisation of these convective systems along a line, as is clearly visible in the radar images (Figure 3a), is due to a strong mesoscale forcing, which provides for a higher degree of predictability than for isolated convection. Indeed, all the models predict this line of precipitation with the correct timing (starting around 2100 UTC), as shown in Figure 6a. However, the simulated rainfall (Figure 8a, b) is slightly displaced closer to the coast, in particular in the C2 forecast, possibly because the orographic uplift is needed to trigger the convection in the model (as will be further discussed in Section 4.4). In agreement with higher values of θ_e in the lower model levels (Figure 7) and, hence, higher convective available potential energy (CAPE) and instability, precipitation develops more upwind with respect to the coast and orography in MOLOCH than in COSMO.

Later on, the rainfall line moves eastwards over the Ligurian Sea (Figure 3b), finally reaching Tuscany at around 0300 UTC. The precipitating system in the model simulations moves more slowly than observed. Moreover, the convective line in MOLOCH moves away from the coast, while intensifying and progressing eastwards towards Tuscany, whereas in COSMO, the precipitation

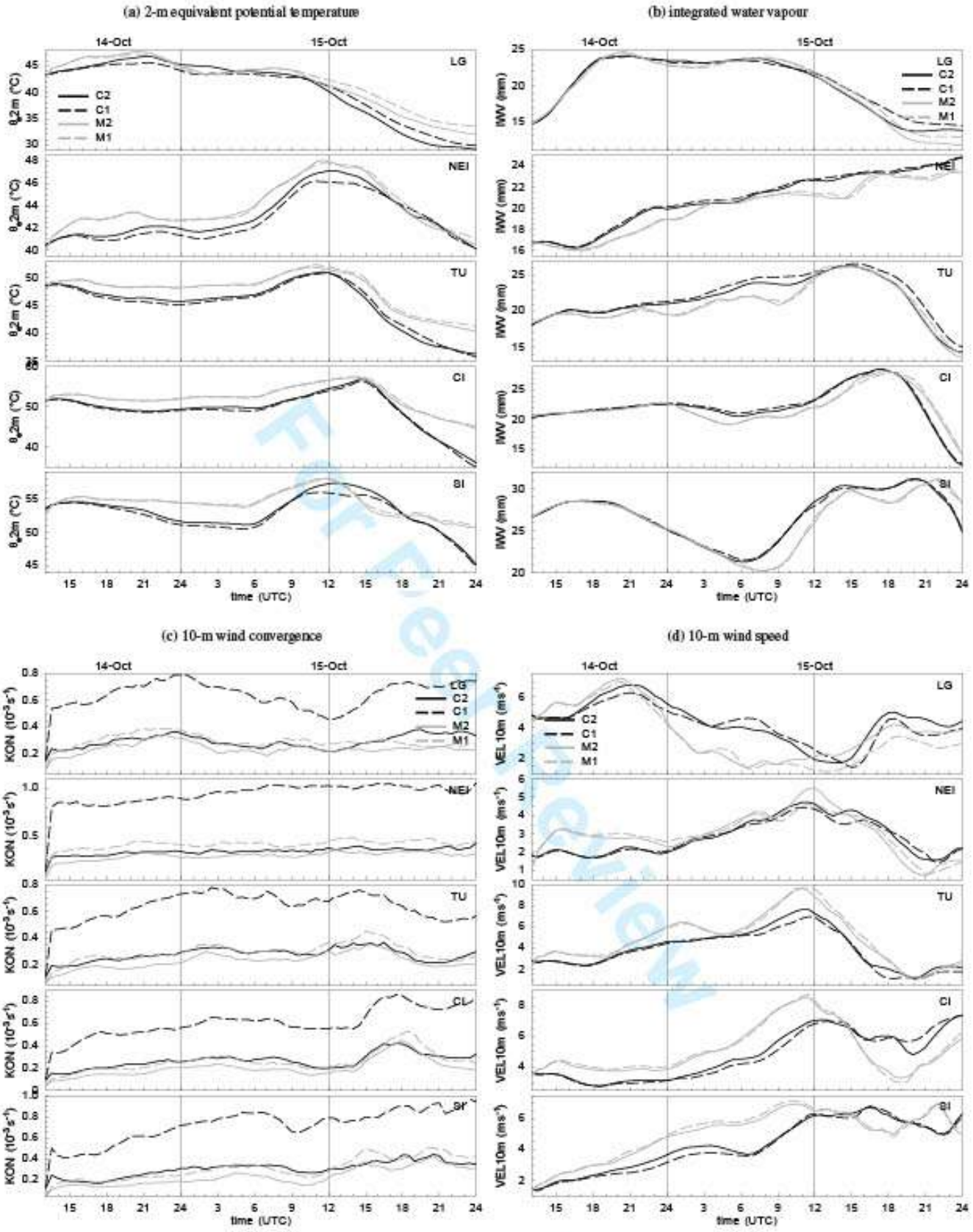

Figure 7. Domain-averaged meteorological parameters for the different boxes depicted in Figure 1. (C2: COSMO 2.8 km; C1: COSMO 1 km; M2: MOLOCH 2.3 km; M1: MOLOCH 1.5 km)

affecting the coastal area of Liguria lasts longer (Figures 8c, d). At around 0300 UTC, in Figure 6c, MOLOCH shows a small peak of precipitation over TU, the underestimation of which is attributed to the fact that the simulated precipitation is intense, but very localised, while over LG (Figure 6a) COSMO produces more intense rainfall in the decreasing phase of the peak. The averaged values of 10-m wind speed (Figure 7) over LG confirm this different behaviour of the models: after 0000 UTC, the decrease

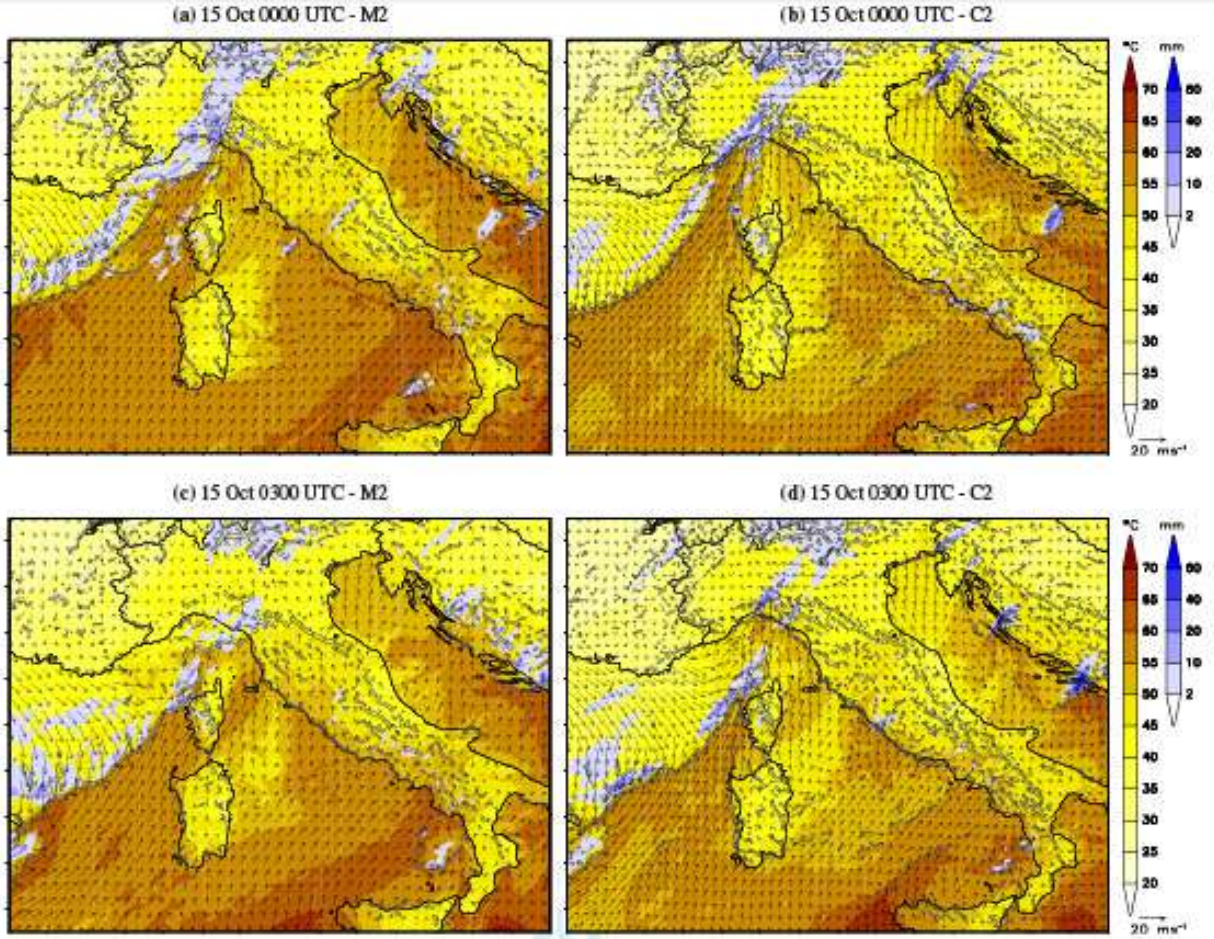

Figure 8. Model forecasts valid at 0000 UTC (a) and (b) and at 0300 UTC (c) and (d), 15 Oct 2012: 10-m wind, 2-m θ_e (red/yellow colour bar), precipitation (blue colour bar) and 10-m wind convergence (solid black line). MOLOCH at 2.3 km (a), (c) and COSMO at 2.8 km (b), (d) horizontal resolution.

of wind speed in MOLOCH is associated with the eastward shift of the convergence line, faster than in COSMO where, on the other hand, southerly intense low-level flow still impinges on the Ligurian Apennines (Figures 8c, d).

This first phase of the event terminates with the development of another precipitating system over the eastern coast of Liguria (second peak in Figure 6a) in correspondence with the warm sector of the approaching frontal system. The convective nature of the precipitation is confirmed by the intense lightning activity recorded in the area around 0600 UTC (see Figure 11 in Ferretti *et al.*, 2014). Although with a slight delay, both models predict this precipitation associated with the front extending from the western coast of Corsica, across the Ligurian Sea, to the northern Apennines.

The second phase of the event is characterised by a less intense large-scale forcing since the convergence line associated with the Mistral (and also the front) somehow loses its organisation while crossing Sardinia and Corsica. Rainfall is mainly triggered by mesoscale convergence patterns, strongly modulated by the interaction of the westerly/southwesterly flow with the complex orography of the islands. The precipitation mainly affects Tuscany during this phase, in particular in the mountainous regions, where convection develops between 0900-1200 UTC fed by the moist low-level southerly flow over the Tyrrhenian Sea. At 1300 UTC, radar images (Figure 3c) clearly show an organised line of convection extending from the Elba Island towards inland Tuscany, which remains almost stationary for several hours, producing high amounts of rainfall. At first glance (Figure 6c), models simulations are quite similar. A first peak of precipitation, remarkably underestimated, is forecast around 0900 UTC associated with southerly flow over the orography, as confirmed by averaged near-surface wind and θ_e (Figure 7) which are steadily increasing in this phase. Later on, another period of intense precipitation produces peaks that are similar in shape and amplitude ~~and just~~ but shifted in time, with MOLOCH simulations producing rainfall earlier than COSMO. However, in spite of this similarity in the area-averaged rainfall, a more detailed investigation of the model forecasts reveals that at this time the

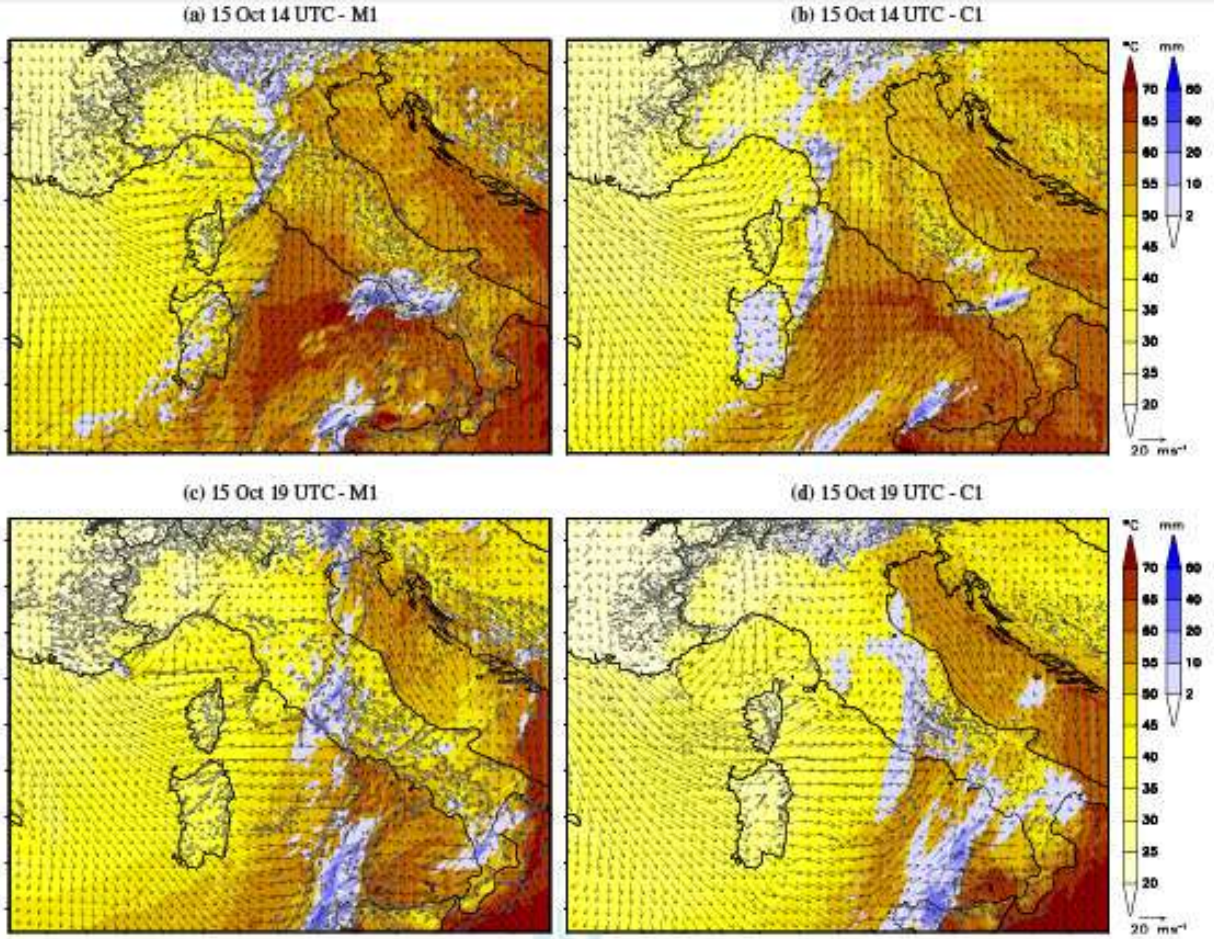

Figure 9. Model forecasts valid at 1400 UTC (a) and (b) and at 1900 UTC (c) and (d), 15 Oct 2012: 10-m wind, 2-m θ_e (red/yellow colour bar), precipitation (blue colour bar) and 10-m wind convergence (solid black line). MOLOCH at 1.5 km (a), (c) and COSMO at 1.0 km (b), (d) horizontal resolution.

two models provide quite different predictions (Figures 9a, b). MOLOCH forecasts a northerly outflow of colder air from the Po valley, confirmed by wind observations in Genoa (not shown) towards the Genoa Gulf and an area of mesoscale convergence developing close to the Elba Island starting from 1300 UTC, where the westerly low-level wind flowing around the northern edge of Corsica converges with a ~~southerly warmer flow over the Tyrrhenian Sea~~ southwesterly warmer flow east of Corsica. The latter is produced by a channeling effect between Corsica and Sardinia and the subsequent northward deflection. Along this convergence line, MOLOCH triggers convection (see also the increasing values of θ_e and convergence averaged over the box in Figure 7) for several hours until the front sweeps over the area. In the COSMO simulations by contrast (Figures 9b, d), the outflow from the Po valley develops later and the frontal system seems to be more defined (with respect to the MOLOCH forecast; Figures 9a, c) over the Tyrrhenian Sea, east of Corsica and north of Sardinia. Moreover, the eastward progression of the front itself seems to be faster in COSMO during the afternoon of 15 October. The orographic deflection of the islands and the convergence area located close to the Elba Island are captured in both COSMO simulations, but rainfall seems to be more associated with the large-scale front rather than with the mesoscale convergence patterns and is produced along an almost continuous band from Tuscany to Sardinia. While the meteorological evolution during this phase remarkably differs in the two models, the impact of the horizontal resolution seems to play a minor role only, with the high resolution runs reproducing a sharper convergence line and associated phenomena slightly more accurately.

The third phase of the event during the afternoon is again characterised by an the important role of large-scale forcing, which is responsible for the frontal convective line reaching central Italy (Figure 3d) and, later, southern Italy as well as for the southeasterly Sirocco wind over the Adriatic Sea, which brings moist air over the eastern Alps. As the front moves rapidly eastwards towards the Italian peninsula, convection is triggered over the southern Tyrrhenian Sea, where MCSs develop along the

frontal edge. In particular, rainfall activity appears to be well-organised along a convective line while moving over the city of Rome (see Figure 10 in Ferretti *et al.*, 2014). The observed sharp peak of averaged rainfall (Figure 6d) is captured by the models and appears to be associated with high values of IWV and low-level convergence (Figures 7b, c). The slight shift in time of the maximum rainfall intensity between the models confirms that in COSMO, the progression of the front is faster than in MOLOCH. The abrupt decrease of θ_e (Figure 7a) in all the simulations reflects the arrival of colder and drier air, which concludes the rainfall event.

More to the south, MCSs develop in the early afternoon already over the Sea (Figure 3c), but are simulated by the models too close to the coast. This produces an overestimation of the box averaged rainfall (Figure 6e). The forecast error may possibly be attributed to the fact that these MCSs develop well ahead of the approaching front and, thus, are not triggered by large-scale forcing, but under locally suitable conditions. For NWP models, it is very difficult to accurately simulate the triggering of this isolated convection, which is usually associated with low intrinsic predictability. On the other hand, the convection that develops later in the evening (Figure 3d) and is triggered directly by the frontal passage is described better in the model simulations.

At the same time, the southeasterly wind intensifies over the Adriatic Sea on the eastern side of the Apennines. Averaged values of θ_e, wind, and IWV in the NEI box (Figure 7) clearly show the warm and moist air masses impinging on the Alps, where direct orographic uplift triggers intense precipitation. Lightning activity reveals the presence of embedded convective activity within the orographic precipitation, quite typical of these type of events (Manzato 2007). Consistently with increasing CAPE, convection develops also along the northern Adriatic coast (Figures 3 c, d). Both models reproduce at the correct time the moist air masses over the Adriatic Sea flowing over the Alpine chain and the associated precipitation that is mainly localised in correspondence with the orography (Figures 9c, d).

As evident from Figure 7, low-level equivalent potential temperatures simulated by COSMO are higher lower than those forecast by MOLOCH for most of the integration period. Since larger values of θ_e coincide with larger values of CAPE (e. g. Kohler *et al.* 2010), this may have important implications for the expected intensity of convection and convective rainfall. The analysis of the 2-m specific humidity reveals that MOLOCH mostly simulates around 0.5-1.5 $\mathrm{g\,kg^{-1}}$ higher values than COSMO (not shown). As the 2-m temperature is rather similar in both models, the relative humidity in the MOLOCH output is 5-8% higher as well and the increase in equivalent potential temperature is solely a result of increased low-level moisture.

Another feature shown in Figure 7 is the strong increase of convergence in the COSMO model when going from 2.8 km to 1 km grid spacing. A convergence increase is also found in the MOLOCH runs, but the jump in resolution (from 2.3 km to 1.5 km) is smaller than for the COSMO simulations. The increase itself when going to higher grid spacing can be explained by the ability of the model to better simulate smaller-scale wind gradients and the terrain-induced flow modification due to the better resolved orographic features. As can be seen in Figure 9, the 1-km COSMO run simulates very localised narrow regions of convergence restricted to small areas, which explains the higher domain-averaged convergence compared to the MOLOCH simulations. Note that the domain averages were computed by just averaging the convergent contributions of the wind divergence.

4.4. *Role of orography*

Atmospheric processes are strongly influenced by the presence and shape of the underlying orography. On local scale, on coastlines of islands or the continent, breezes driven by differential heating between land and sea can lead to convection initiation. Furthermore, mountainous terrain can influence atmospheric flow on the mesoscale through lifting, flow deviation or blocking. Hence, it has a strong impact on the development of precipitating convection (e. g. Barthlott and Kirshbaum 2013). To study the influence of the orography on convective precipitation for IOP 13 and to verify the results described in the previous sections, three additional experiments were performed with the COSMO and MOLOCH models at a horizontal resolution of 2.8 km and 2.3 km, respectively:

1. terrain elevation in the entire model domain is restricted to 10 m (hereinafter referred to as FLATGLOBAL),

Table 4. 35-h accumulated precipitation for the different boxes in 10^9 ltr (only land points).

name	LG	NEI	TU	CI	SI
C2 REF	1217	2013	493	544	998
M2 REF	1174	1854	594	680	1129
C2 FLATGLOBAL	467	504	522	473	438
M2 FLATGLOBAL	904	1122	445	313	733
C2 FLATISL	1146	2021	541	584	1064
M2 FLATISL	1094	1993	614	695	1177
C2 NOISL	1108	2002	669	625	1044
M2 NOISL	1046	1968	831	754	1201

2. terrain elevation of the islands of Corsica and Sardinia is restricted to 10 m (hereinafter referred to as FLATISL),
3. the islands of Corsica and Sardinia are removed completely (hereinafter referred to as NOISL).

The terrain modifications were conducted by modifying the external orography data file of each model prior to the model run. The preprocessor of the models extrapolated the atmospheric fields of the large-scale model to the high-resolution grid, as usually done in the nesting procedure, but with the new orography height. When the islands were removed completely, the corresponding grid points were defined as sea points and the sea surface temperature of the surrounding sea was used to fill the gap. However, the models adjusted to the new orographic conditions quickly, in approximately 2-3 h.

Results in Figure 10 (to be compared with (Figures 5a, c) show that the intense precipitation along the French and Italian coast during the evening of 14 October is completely missing in the FLATGLOBAL experiment, where the Alpine chain is flattened. This result confirms that the convection during this initial phase of the event is triggered by the coastal orography: its blocking effect on the impinging moist flow from the Mediterranean Sea produces a pronounced convergence line almost parallel to the coast. Only later during the night, the FLATGLOBAL experiments, in particular the MOLOCH simulation, produce rainfall over LG, although the intensity is weaker and the pattern is shifted westwards compared to the reference simulation. However, the total amount of rainfall over LG is remarkably weaker than in the reference run (REF, Table 4). Later, during the night of 14 October and in the first hours of the following day, the predicted rainfall moves from LG to TU. It seems that the coastal orography only plays a secondary role in this phase in determining the precipitation field, while the key forcing mechanism is provided by the frontal system progressing over the Ligurian Sea. However, the Mistral outbreak and the eastward progression of the front occur more slowly with flat orography than with realistic orography. Once the front reaches Corsica in the early morning, an intense northerly current penetrates into the Mediterranean basin due to the absence of the Alpine barrier. From here on, the simulation results are too far from reality to be of any use.

The other two experiments, with the Alpine orography being unchanged, are used to investigate the development of precipitating systems especially in the following phase of the event, when the islands of Corsica and Sardinia directly interact with the southwesterly flow. In fact, the initial phase is nearly identical for the control run with unchanged orography (REF), FLATISL, and NOISL, and differences are found only in the evolution during 15 October. In particular, maps of total precipitation (Figure 10) show that these differences are mostly relevant over TU, where the sensitivity experiments simulate a much larger amount of rainfall. Over CI, SI, and over the Alps, the differences seem to be more associated with slight displacements of precipitation patterns. Anyway, the evolution of area-averaged precipitation displayed in Figure 11 allows for a more precise investigation, together with low-level wind and temperature, and precipitation (not shown).

Over LG, the forecasted rainfall only exhibits small differences among the REF, FLATISL, and NOISL experiments, mainly occurring in the late morning of 15 October, and the total precipitation over the area (Table 4) is almost the same. After the passage of the main front, the reduced or even absent interaction of the southwesterly flow with the islands in the two sensitivity experiments FLATISL and NOISL moves the main rainfall area quickly over TU. In the REF run, by contrast, some rainfall still persists further west over Liguria, especially in the MOLOCH simulation. The moist southwesterly flow directly impinging on the coastal orography of TU in the FLATISL and NOISL runs produces a ~~remarkable~~ marked increase of the area-averaged precipitation over this area (Table 4). Figure 12 shows in more details the dynamical impact of the islands on the low-level flow and on the precipitation in the three sensitivity experiments. At

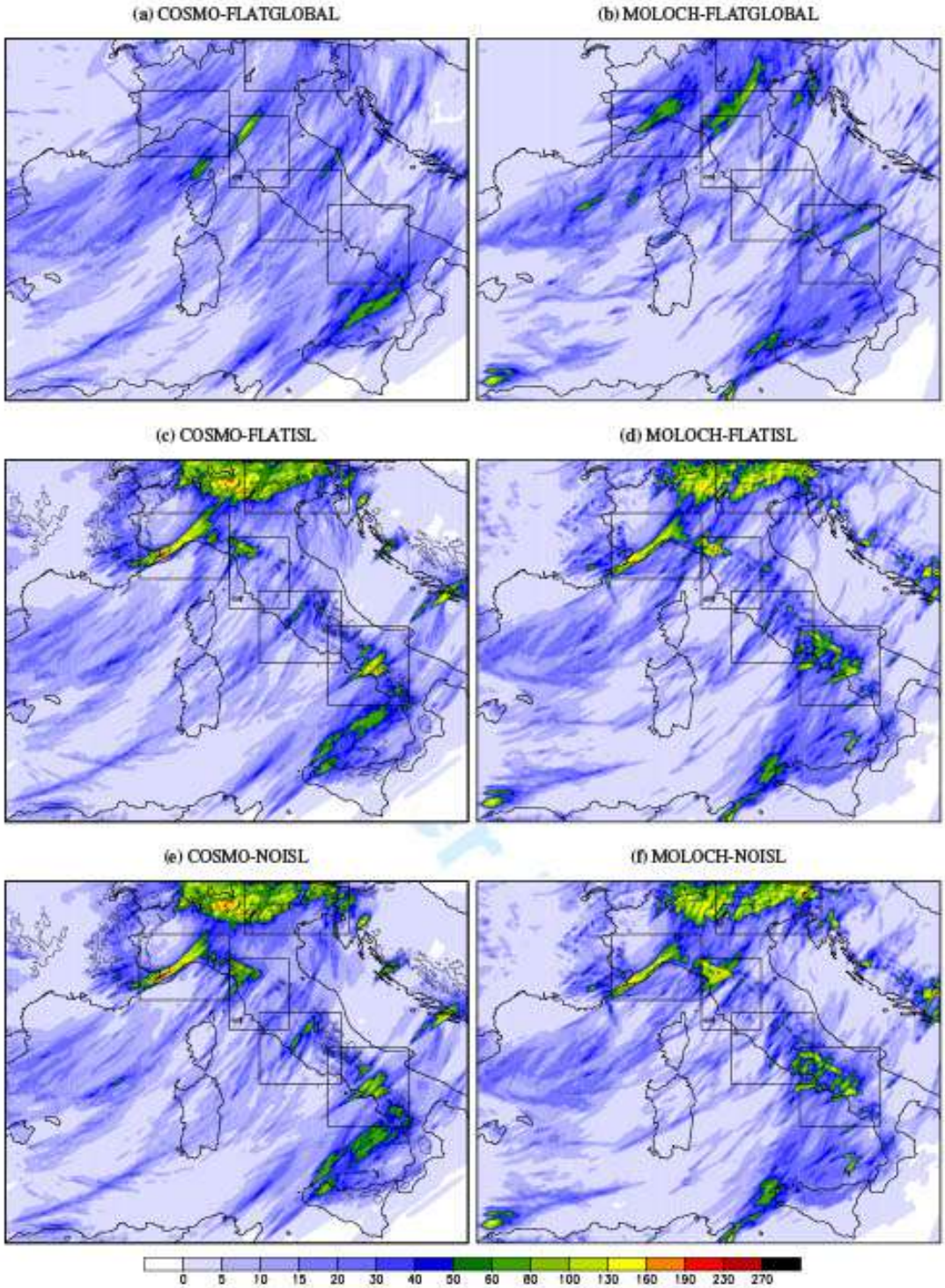

Figure 10. 35-h precipitation amount.

0600 UTC on 15 October, the surface front apparent in the 10-m convergence field, is approaching Corsica. The interaction of the low-level flow with the orography (in the REF only) produces a complex pattern of convergence above both islands. Moreover, it is responsible for triggering some weak rainfall in the northwestern part of the Corsican island. Ahead of the front in the NOISL run, the southwesterly low-level wind flows undisturbed over Corsica, thus producing a convergence line oriented in a southwest-northeast direction, between the island and the TU coast. Precipitation is associated with this line over the sea, but the most intense phenomena are localized over the TU area, where the orographic forcing of the Apennines further enhances the vertical motions. In the FLATISL run, the low-level convergence along the western Corsica coast indicates that the interaction with the ground is slowing down the low-level wind. However, although to a less extent, the low-level flow is able to impinge directly on the Apennines, producing moderate rainfall over TU. On the other hand, the real orography in the REF experiments

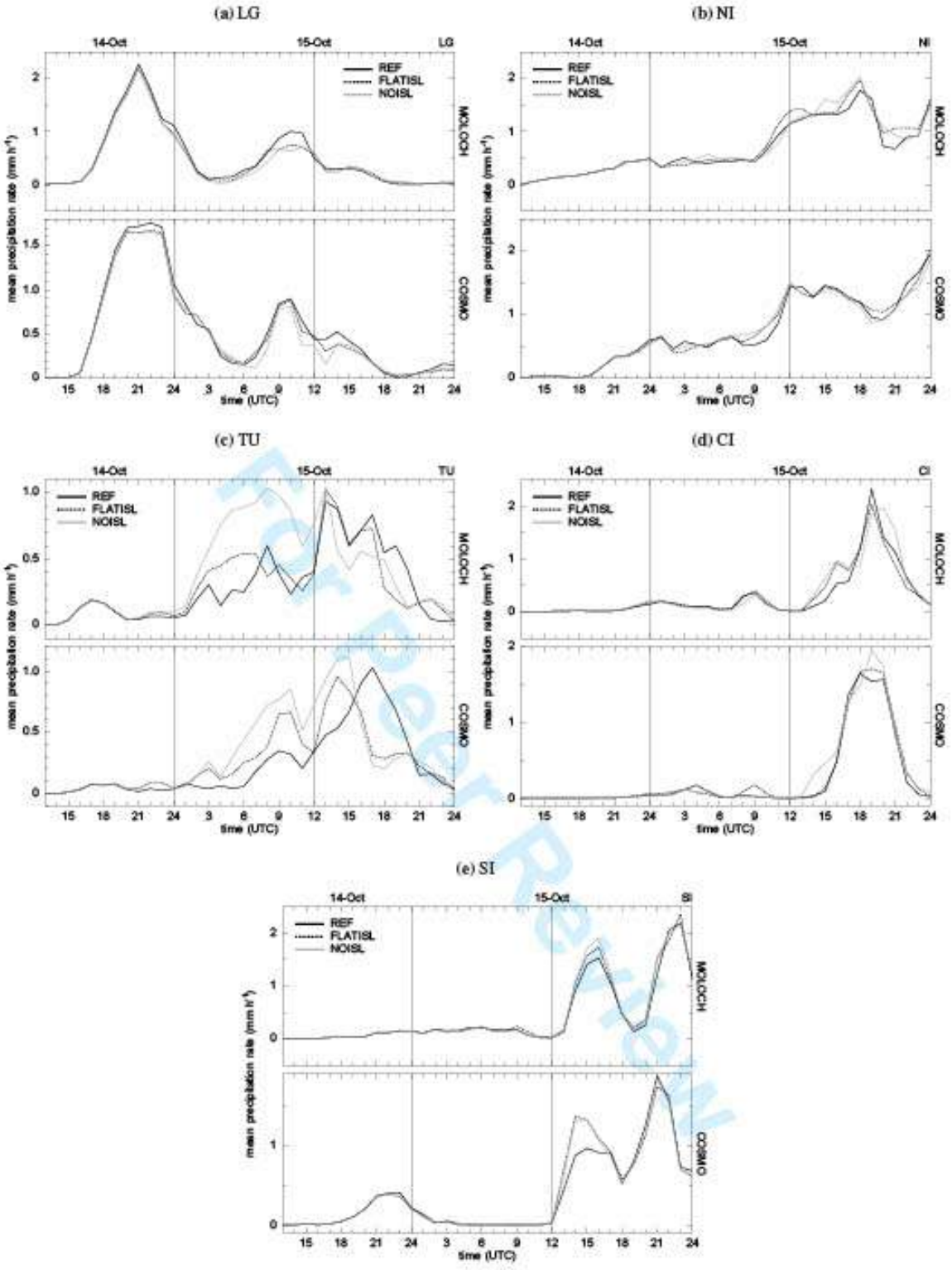

Figure 11. Spatially averaged precipitation for COSMO and MOLOCH.

prevents the moist pre-frontal flow to reach TU during this phase. It turns out that the The total amount of precipitation progressively increases when the sheltering effects of the islands is reduced, while the temporal evolution of rainfall is only slightly modified (Figure 11). This behaviour is observed consistently in both MOLOCH and COSMO simulations. Later on, in the morning of 15 October, rainfall intensity over TU progressively increases. Rainfall is systematically more abundant in NOISL. In the REF run, the low-level moist flow is disturbed on the lee side of Corsica, preventing the southerly flow over the Tyrrhenian Sea from converging with the main pre-frontal southwesterly current directly on the Apennines. After 1200 UTC, the differences tend to decrease, although the rainfall peak in the COSMO sensitivity runs occur earlier than in REF. However, in spite of a similar

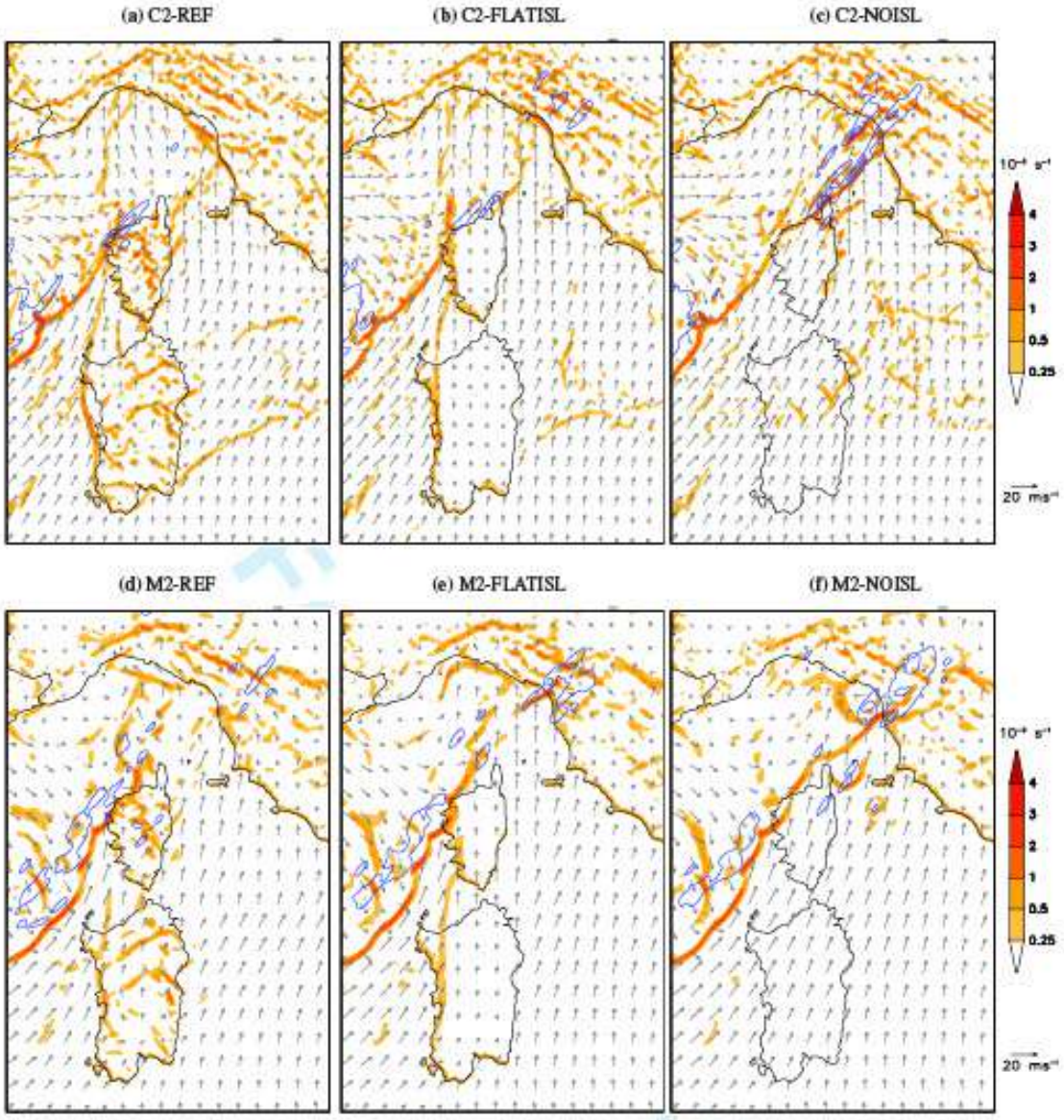

Figure 12. 10-m wind convergence (colour shading), 1-h precipitation in mm (blue contours at 5 and 20 mm), and 10-m wind vectors at 0600 UTC on 15 Oct 2012 for COSMO (a-c) and MOLOCH (d-f).

mean precipitation over TU, the rainfall field in the REF run is characterised by some patterns of convection over the sea, missing in the sensitivity runs, where low-level convergence is produced as a consequence of flow deviation around the islands.

Once the front progresses eastwards, the experiments become very similar and only small differences can be detected for the rainfall event over CI in the evening, where the convection is triggered by the large-scale forcing provided by the front. In NOISL and FLATISL, precipitation starts slightly earlier than in the REF run, but the timing of the most intense rainfall is almost identical. However, some differences in rainfall location result, as is shown in Figure 10. In this area, total precipitation slightly increases when removing the upstream orographic obstacle, but to a much lesser extent than over TU. The sheltering effect of the islands is less pronounced and the precipitation is mainly related to the passage of the frontal system, producing a large-scale forcing.

Finally, it is worth mentioning that precipitation over Corsica, which is forecasted mainly on the windward side of the island orography in the REF run, is remarkably reduced in FLATISL and almost negligible in NOISL. This suggests that rainfall is produced by direct uplift of the prevailing southwesterly currents affecting the central Mediterranean area.

To sum up, the sensitivity experiments provide some interesting information. Similar sensitivities are obtained with COSMO and MOLOCH. First, these experiments confirm the importance of large-scale/mesoscale forcing to rainfall triggering in two different phases of the IOP: at the beginning of the event, the orographic

blocking and uplift are responsible for heavy rainfall in LG; later, the frontal system triggers convection over CI. The organisation of the precipitation systems during these phases results from a relatively large-scale forcing and, hence, can be simulated by the models more easily. On the other hand, the interaction between the frontal system and the associated low-level flow with the orography of Corsica and Sardinia, is responsible for the intensity and location of rainfall during the whole morning and early afternoon of 15 October. In fact, the experiments clearly reveal that the islands shelter the Italian coastal regions and flow deflection is the key mechanism modulating the rainfall distribution, since it determines: i) small-scale complex patterns of low-level convergence over the sea in the lee of Corsica, where convection can be triggered; ii) the location of interaction and orographic uplift, where the undisturbed low-level flow is able to reach the Apennines.

4.5. *Vertical structure of the atmosphere*

To analyse in more detail the model performance in terms of correct simulation of relevant processes, we compare the predicted vertical structure of the atmosphere with observations, made for the HyMeX SOP 1. First, model profiles corresponding to the location of the synoptic radiosonde station of Ajaccio on the southwestern coast of Corsica (see Figure 1a) are investigated. It is worth noting that the upstream location of Corsica is suitable for studying the characteristics of the flow leading to high-impact weather over Italy.

At 0000 UTC on 15 October, the radiosonde observations processed at high resolution for the SOP 1 (Figures 13a, c) show a moist-neutral layer of air from the ground to approximately 930 hPa, followed by an almost saturated atmosphere up to the level of 650 hPa. Both COSMO realisations (Figure 13a) simulate a similar stratification, but the temperature and dewpoint temperature are slightly too high in the lowest levels. A moist layer of air is also simulated, but the dewpoint depression is higher than in the observations. The MOLOCH runs (Figure 13c) simulate even warmer (dewpoint) temperatures near the ground and only a shallow layer of humid, almost saturated air between 900 and 850 hPa. In the lower layers, the differences of the different resolution models appear to be almost negligible. Above 650 hPa, measurements indicate drier conditions through the entire troposphere, except at the level just above 500 hPa, where the dewpoint temperatures increase indicates more humid air. In the middle troposphere, the C2 run simulates this drier region in good agreement with observations, although the dewpoint increase at 480 hPa is less pronounced. The run with 1 km grid spacing simulates a moister profile than the C2 run, with the humidity decreasing with height, and does not reproduce the observed local dewpoint increase above 500 hPa. A drier middle troposphere is also captured well in the MOLOCH simulations, although the drier layer is placed at a lower altitude in both M2 and M1 runs, compared to the observations. However, the humid layer near 480 hPa is simulated well by both model configurations. At higher levels up to the tropopause, MOLOCH simulates a too moist atmosphere, while COSMO agrees with the radiosonde observations. The southeasterly wind near the ground is captured partly by C2 only, whereas the observed rotation of the wind direction with increasing altitude and intense southwesterly winds at higher levels is captured well.

At 1200 UTC on 15 October, the radiosonde measurements still show a nearly neutral boundary layer up to a level of 900 hPa and an almost saturated atmosphere up to 700 hPa. At this time, the middle and higher troposphere remains equally humid, although not saturated. Both COSMO runs capture the vertical profile very well from the lower levels up to 700 hPa. However, the simulated profiles are too dry near the ground, especially for C2, and slightly too moist in the middle troposphere, although there is a rather good agreement with the observations. Above the PBL, the atmosphere is more or less moist-neutral throughout the entire troposphere as a result of the convective rain band passing Corsica associated with the frontal system. Similar results hold for the MOLOCH runs. Although the dewpoint temperatures near the ground for both MOLOCH runs are closer to the observations than for the COSMO runs, a dry bias is still present. The near-surface winds are not simulated by any of the models. The (south)westerly winds above, however, are simulated well, but again with weaker wind speeds than observed.

To sum up, both models simulate the atmospheric stratification for most of the troposphere reasonably well. Differences occur primarily in the PBL which is too dry in the simulations.

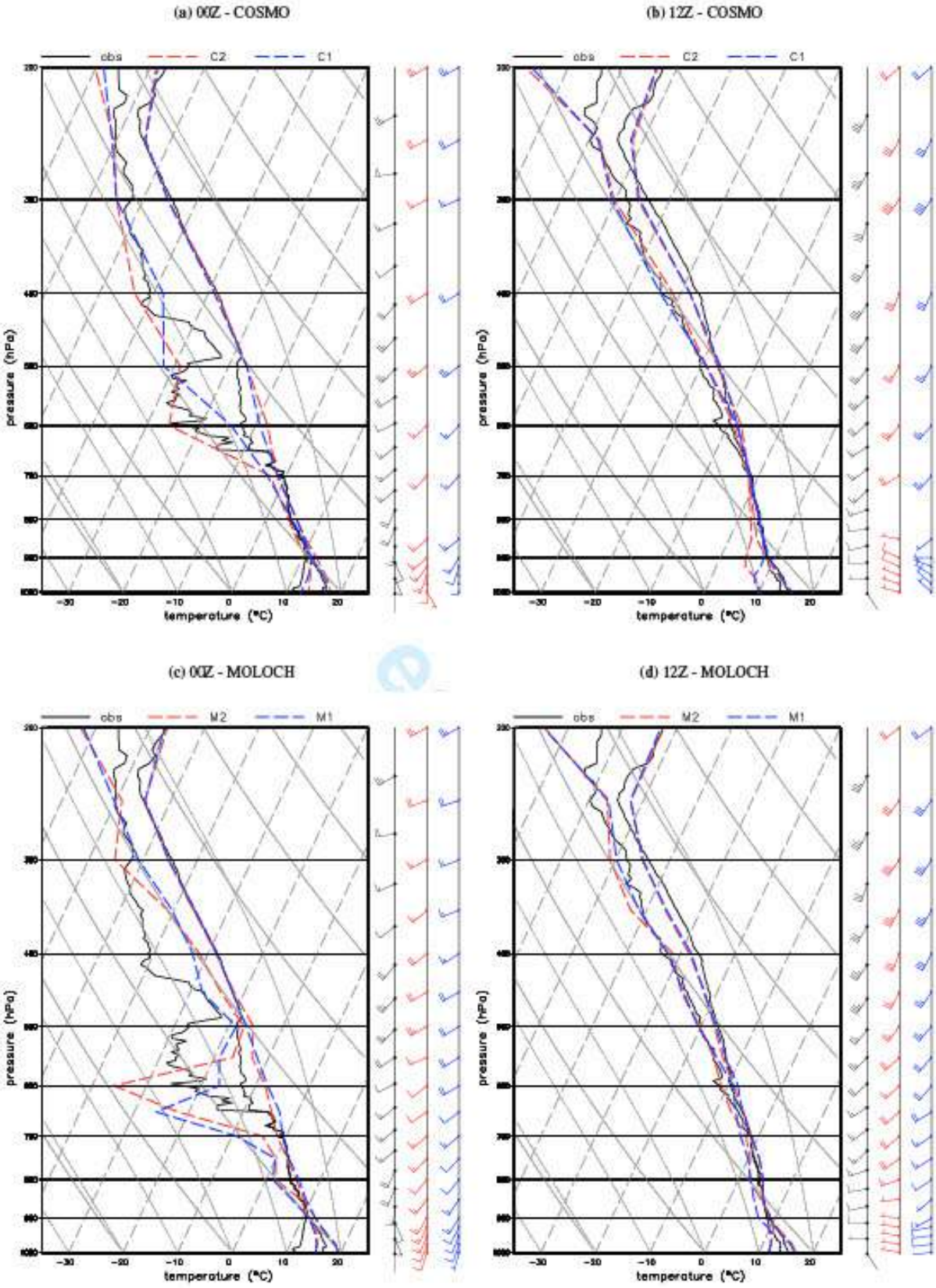

Figure 13. Tephigram of simulated and measured vertical profiles at Ajaccio on 15 October 2012.

Furthermore, there are only small differences between the individual model runs at the two different resolutions. Possibly, the higher horizontal grid spacing alone is not sufficient and also a higher number of vertical levels might be needed to improve the model representation of the vertical structure of the atmosphere and of the local effects determining the low-level wind in such a complex region.

The availability of additional observations made during the HyMeX SOP 1 field campaign enables us to perform a more profound validation of our numerical simulations. During IOP 13,

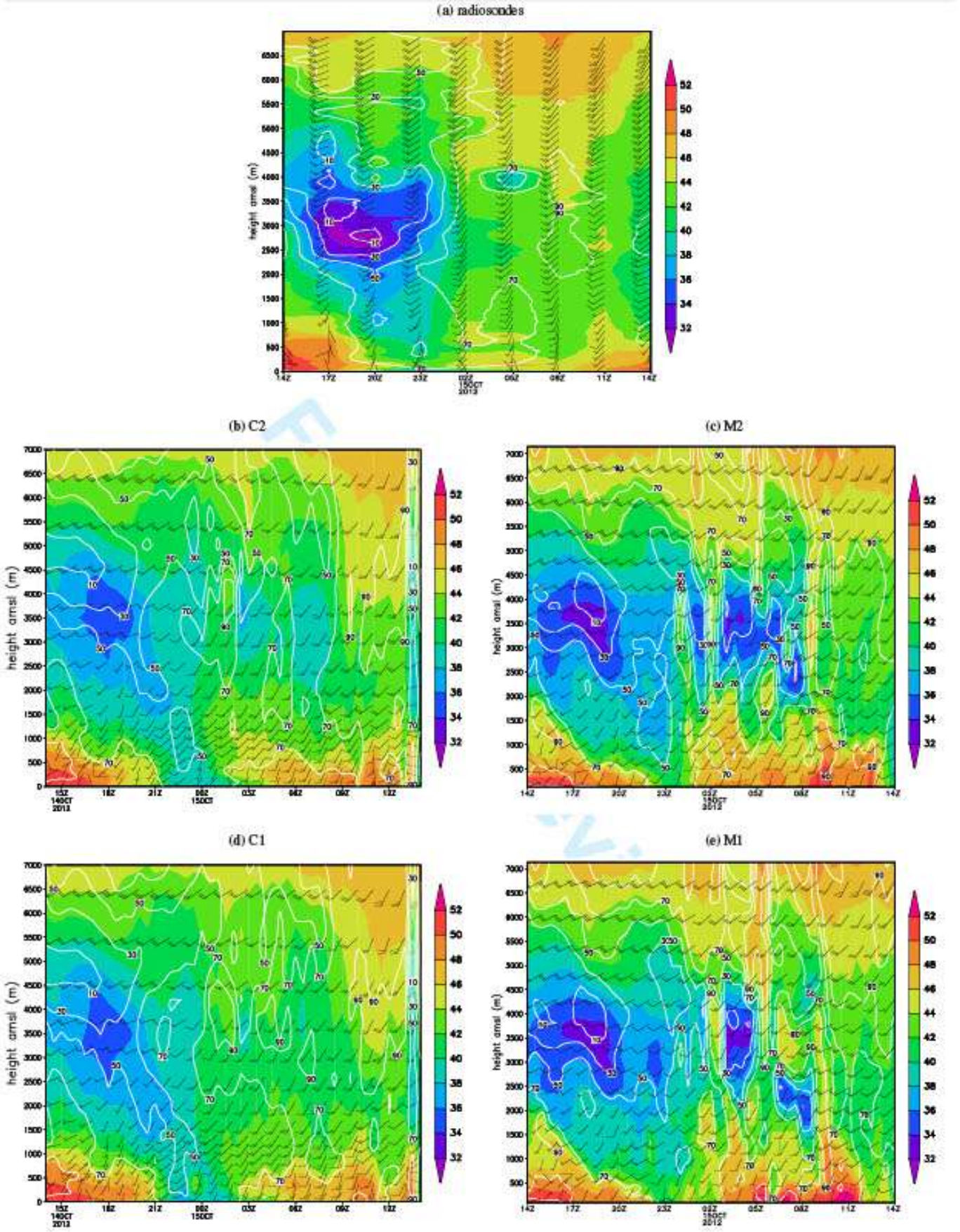

Figure 14. Time-height cross-sections of equivalent potential temperature (colour shading, in °C), relative humidity (white contours, in %), and horizontal winds (barbs, in kn) at San Giuliano on the eastern coast of the Corsican island.

radiosonde measurements were performed near the eastern coast of Corsica at San Giuliano (see location in Figure 1a) from 14 October 1400 UTC until 15 October 1400 UTC with a frequency of 3 h. This allows for comparing time-height cross-sections from radiosonde measurements and numerical simulations as presented in Figure 14. The most pronounced feature in the radiosonde

observations is the arrival and descent of air with progressively colder equivalent potential temperatures from 1400 UTC to 2000 UTC on 14 October. The core of cold air is located at an altitude between 2500 m and 3000 m amsl. With a relative humidity of less than 10%, the air is particularly dry, especially when considering this low height range. After 2300 UTC, the wind slightly turns to a southwesterly flow (even southerly near the ground) with increasing wind speeds and warmer equivalent potential temperatures associated with the pre-frontal flow (Figure 8). The instability is highest at the beginning of the analysed period whereas there is only a small vertical gradient of θ_e starting from 0200 UTC on 15 October. The signature of the frontal passage is not very clear from this time-height cross-section: whereas a veering wind shift accompanied by an increase of wind speed is observed at 0800-1100 UTC on 15 October, the equivalent potential temperature field shows similar or rather increasing values, especially at low levels. The location of San Giuliano on the lee side of the island orography, the elevation of which exceeds 2700 m, certainly inhibits the effects of the approaching cold front on the near-surface temperature and humidity structure. Veering of the wind and slightly colder temperatures are observed at higher altitudes.

The model simulations show some differences with respect to the observations, which depend on the model (COSMO or MOLOCH) but also on the configurations of the specific model. First, the warm low-level temperatures at the beginning of the period as well as the progressive descent of colder air are captured well by all simulations. However, none of the models is able to predict equivalent potential temperatures below 32 °C as observed by the radiosondes. The region with lower temperatures reaches closer to the ground in COSMO than in MOLOCH runs. After 0000 UTC on 15 October, M2 simulates very sharp gradients of relative humidity, possibly due to localised convective activity. As obvious from the veering wind shift, the timing of the frontal passage on the eastern coast of Corsica is similar for C2 and M2 (around 1000 UTC). Both models simulate a decay of convective rain off the eastern coast. A unique feature of both COSMO runs is the abrupt decrease of relative humidity from the ground to 7000 m amsl between 1300 UTC and 1400 UTC on 15 October. The results from C1 and C2 are very similar, except that θ_e values between 2500 and 4500 m asl are slightly warmer in the C1 run and, hence, closer to observations. Both MOLOCH runs simulate warmer low-level temperatures on 15 October. The increased instability at this grid point could be the reason for the strong humidity gradients simulated above.

Furthermore, the radiosonde observations reveal no land breeze during the night and early morning of 15 October and the low-level flow comes from south-east. All models simulate southwesterly winds at that location during the night, indicating that the impact of the island on the near-surface winds is not represented well in any of the models. Note that the maximum elevation of Corsica is 2710 m amsl, whereas it is 1906 m and 2306 m for COSMO (C2 and C1, respectively) and 1848 m and 1960 m for MOLOCH (M2 and M1, respectively). As a result, the topographic influence of the land mass in the simulations is weaker than in reality.

The extra-soundings performed at Udine-Campoformido WMO station (see Figure 1a) for the SOP 1 allow for a similar comparison in a completely different area of the simulation domain, where weather evolution is modulated mainly by intense low-level southerly flows (namely, Sirocco) driving warm and moist air masses towards the Alpine chain, where most of the precipitation is recorded on 15 October. The soundings clearly show the warm and humid air entering the eastern Po valley (Figure 15), although a weak north-easterly flow persists close to the ground. This is the signature of a barrier wind caused by the blocking effect of the orography, which is often observed at the foothills of the Alps during intense precipitation episodes (Buzzi 2004). The model simulations correctly reproduce the evolution of the atmospheric profile and the southerly advection of air, including the low-level blocking. While the southerly flow impinging on the Alps produces a warmer θ_e than observed in the lower layers, the colder air progression at around 3000 m altitude is predicted well by all models. C2 and C1 results are very close to each other and both display the signature of convective activity, as a result of which humidity is increased locally. Low-level winds are slightly overestimated, while the thermodynamic evolution aloft is reproduced accurately. M2 and M1 differ in the intensity of the low-level warm advection at around 1200 UTC, 15 October, with the M2 simulation being characterised by stronger winds

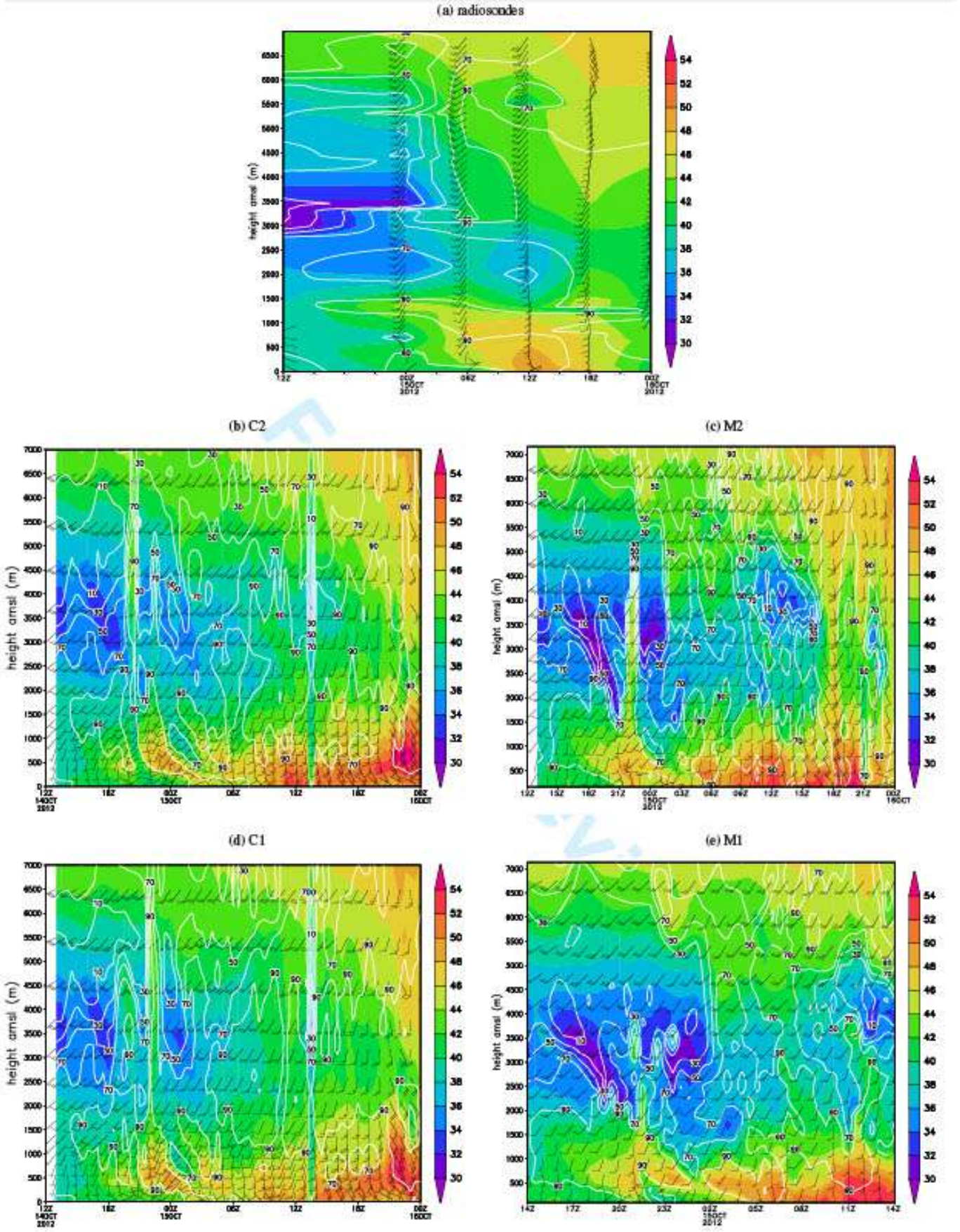

Figure 15. Time-height cross-sections of equivalent potential temperature (colour shading, in °C), relative humidity (white contours, in %), and horizontal winds (barbs, in kn) at Udine.

and higher θ_e values. M1 seems to be in better agreement with observations. However, both MOLOCH runs simulate a colder atmosphere at the end of the event.

5. Summary and discussion

This study presents numerical simulations with two convection-permitting models (COSMO and MOLOCH) driven by the same

initial and boundary data for the Intensive Observation Period 13 (14 and 15 October 2012) of the first HyMeX Special Observation Period (SOP 1). During this IOP, heavy precipitation affected southwesterneastern France and several parts of Italy, with observed maximum rain rates of 114 mm h^{-1}. The synoptic-scale forcing during this event was quite ~~remarkable~~ strong due to an approaching upper-level trough and the associated cold front, together with a strong Mistral outbreak in the western Mediterranean basin. Nevertheless, mesoscale features, such as the interaction of the flow with the orography, played an important role as well. Model simulations were initialised on 14 October at 1300 UTC (integration time 35 h) and also on 15 October at 0000 UTC (integration time 24 h) to cover the entire event and to further assess the influence of forecast lead time. However, no notable differences in precipitation amount and timing were found, with the exception of a slightly improved rainfall prediction over the Alps and a slightly faster progression of the front (only in MOLOCH) in the simulations initialised later. This allows the conclusion to be drawn that due to the strong synoptic-scale forcing, at least the large-scale features are characterised by a sufficiently large degree of predictability and that inaccuracies resulting from initial errors and forecast uncertainties do not exclude the use of the longer model integrations for the detailed analysis of this precipitation event.

By using two horizontal grid spacings (COSMO: 2.8 km/1 km; MOLOCH: 2.3 km/1.5 km), the influence of increasing model resolution on the simulation of the event was assessed. Results showed that this influence was rather weak, although the higher resolved runs resulted in a higher correlation of the total rain amount with rain gauge observations. The total rain amount, however, did not increase with model resolution. Also, vertical profiles were broadly similar at both resolutions. The strongest response to model resolution was found to be the increase of low-level wind convergence, in particular for the COSMO model. It must be stated that the number of vertical levels was kept constant in order to investigate the effect of horizontal grid spacing alone.

A detailed analysis of the spatial distribution and temporal evolution of convective precipitation over different areas of the Italian territory revealed a quite satisfactory performance of both models. Differences among the simulations and uncertainties with respect to the available observations were identified and analysed in order to investigate the convective initiation mechanisms in different regions. This synergistic use of the models proved to be very useful for obtaining a better understanding of the processes leading to heavy precipitation and for identifying model deficiencies which prevented a proper simulation of the events. The main model deficiencies were: (i) the displacement of the elongated precipitiation area over Liguria, (ii) the underestimation of precipitation intensity, or (iii) a boundary layer too dry than observed. Different phases during IOP 13 were identified, during which large-scale and local forcing played different roles. Low-level thermodynamic fields as well as total moisture contents, were also examined to verify the analysis.

During the afternoon and night of 14 October, for example, radar observations revealed the presence of a convective line along the coast from south~~western~~eastern France towards Liguria located 20-30 km offshore. All model simulations predicted a similar elongated area of precipitation, but placed it along the coastline or even just inland in the lower-resolution simulations. This indicated that the orographic forcing (uplift) and the land-sea contrast needed to initiate deep convection were represented in the model simulations, but uncertainties still remained, which prevented the correct description of the orographic blocking effect on the impinging moist low-level flow. Increasing resolution only partly alleviated the forecast error.

Furthermore, the COSMO model failed to predict a convective rain event with moderate intensity over the Apennines in central Italy. The comparison with the successful MOLOCH simulation revealed that slightly more stable conditions in the lower levels of the atmosphere in the COSMO model led to a different interaction between the moist flow and the Apennines orography. While in COSMO, the low-level flow was deflected northwards along the coast, the MOLOCH runs produced a moist flow coming from the sea, which was characterised by higher Froude numbers, and rising over the mountain chain, where convection was triggered. These results demonstrate the high importance of correctly resolving the thermodynamic structure of the atmosphere in order to account for the flow modification by interaction with the steep orography.

To further examine the role of the orography, simulations were performed with no mountains (i.e. maximum terrain height restricted to 10 m in the entire simulation domain), flat Corsica and Sardinia islands (i.e. 10 m height orography only over islands), and without islands. The sensitivity of both models to modified orography was very similar and these experiments ~~allowed to highlight~~ highlighted the mesoscale processes that played an important role in triggering convection during the different phases of IOP 13. These experiments confirmed that the orographic blocking and uplift were responsible for the development of the heavy rainfall line in Liguria, since convection was not triggered when the Alpine orography was flattened. Moreover, they showed how the islands of Corsica and Sardinia significantly affected the low-level wind field and temperature/moisture distribution upstream of the Italian regions, where high-impact weather events occurred. The sensitivity experiments clearly revealed that the islands sheltered the Italian coastal regions and that the flow deflection was the key mechanism modulating the rainfall distribution since it determined: i) small-scale complex patterns of low-level convergence over the sea in the lee of Corsica, where convection was triggered and ii) the location of interaction and orographic uplift, where the undisturbed low-level flow was able to reach the Apennines.

Comparison of the model output to radiosonde measurements taken on both the western (Ajaccio) and eastern (San Giuliano) coast of Corsica as well as over north-eastern Italy (Udine) revealed that the overall vertical structure of the atmosphere was reasonably well simulated by both COSMO and MOLOCH. However, it also showed that some relevant differences from observations may occur in the boundary layer, where the detailed orographic effects on the low-level wind field were not represented well. Probably, even higher model resolutions would be required, not only for the horizontal grid, but also for the vertical levels. However, the possible influence of increasing the vertical resolution is left to future work.

Although the influence of an increased model resolution was rather weak with respect to the 24-h precipitation amount, the higher correlation coefficients indicate the potential benefits of higher grid spacing for operational NWP especially for better resolving the mesoscale interaction of the low-level flow with the complex orography that characterises the Mediterranean basin. This interaction is not only limited to direct uplift or flow deviation, but includes sheltering effects on the downstream area as well as generation of localised convergence on the lee side, even far from the islands, which can trigger convective activity. The benefits of increasing horizontal resolution are supposed to be even larger for meteorological situations with weak or moderate synoptic-scale forcing. Finally, we would like to point out that a single case study performed herein is not sufficient for statements to be made with respect to the model's performance in general (especially not for a systematic model evaluation). However, it demonstrates the advantages of having an ensemble of simulations from different state-of-the-art NWP models for process studies.

Acknowledgements

This work is a contribution to the HyMeX international programme. The authors thank Météo France and the HyMeX programme for supplying the data, sponsored by Grants MISTRALS/HyMeX and ANR-11-BS56-0005 IODA-MED project. The authors wish to thank Dr. Mathieu Nuret for rain gauge data, Dr. Alexis Doerenbecher for Ajaccio high-resolution soundings, Martin Kohler for San Giuliano soundings, all available on the HyMeX SOP 1 database. Airborne data were obtained using the ATR-42 Environment Research Aircraft operated and managed by Service des Avions Français Instrumentés pour la Recherche en Environnement (SAFIRE), which is a joint entity of CNRS, Météo France and CNES. The SAFIRE staff is thanked for their support during the SOP 1. The authors acknowledge Cyrille Flamant, PI of the LEANDRE 2 water vapour lidar system.

References

Baldauf M, Seifert A, Förstner J, Majewski D, Raschendorfer M. 2011. Operational convective-scale numerical weather prediction with the COSMO model: description and sensitivities. *Mon. Wea. Rev* 139: 3887–3905, doi:10.1175/MWR-D-10-05013.1.

Barthlott C, Adler B, Kalthoff N, Handwerker J, Kohler M, Wieser A. 2014. The role of Corsica in initiating nocturnal offshore convection. *Q. J. R. Meteorol. Soc.* doi:10.1002/qj.2415.

Barthlott C, Burton R, Kirshbaum D, Hanley K, Richard E, Chaboureau JP, Trentmann J, Kern B, Bauer HS, Schwitalla T, Keil C, Seity Y, Gadian

A, Blyth A, Mobbs S, Flamant C, Handwerker J. 2011. Initiation of deep convection at marginal instability in an ensemble of mesoscale models: a case-study from COPS. *Q. J. R. Meteorol. Soc.* **137** (S1): 118–136, doi: 10.1002/qj.707.

Barthlott C, Kirshbaum D. 2013. Sensitivity of deep convection to terrain forcing over Mediterranean islands. *Q. J. R. Meteorol. Soc.* **139**: 1762–1779, doi:10.1002/qj.2089.

Bech J, Pineda N, Rigo T, Aran M, Amaro J, Gayà M, Arús J, Montanyà J, van der Velde O. 2011. A Mediterranean nocturnal heavy rainfall and tornadic event. Part I: Overview, damage survey and radar analysis. *Atmos. Res.* **100**: 621–637, doi:10.1016/j.atmosres.2010.12.024.

Bennett LJ, Browning KA, Blyth AM, Parker DJ, Clark PA. 2006. A review of the initiation of precipitating convection in the United Kingdom. *Q. J. R. Meteorol. Soc.* **132**: 1001–1020, doi:10.1256/qj.05.54.

Billet S, Toro EF. 1997. On WAF-type schemes for multidimensional hyperbolic conservation laws. *J. Comput. Phys.* **130**: 1–24.

Bruneau D, Quaglia P, Flamant C, Meissonnier M, Pelon J. 2001. Airborne Lidar LEANDRE II for Water-Vapor Profiling in the Troposphere. I. System description. *Appl. Opt.* **40**: 3450–3461.

Burton RR, Gadian A, Blyth AM, Mobbs SD. 2013. Modelling isolated deep convection: A case study from COPS. *Meteorol. Z.* **22**: 433–443, doi: 10.1127/0941-2948/2013/0408.

Buzzi A. 2004. Heavy precipitation and Alpine orography. Proc. Intern. Workshop on timely warnings of heavy precipitation episodes and flash floods, Ljubljiana, 21-22 October 2004, 12pp.

Buzzi A, Davolio S, Malguzzi P, Drofa O, Mastrangelo D. 2014. Heavy rainfall episodes over Liguria in autumn 2011: numerical forecasting experiments. *Nat. Hazards Earth Syst. Sci.* **14**: 1–16, doi:10.5194/nhess-14-1-2014.

Doms G, Förstner J, Heise E, Herzog HJ, Mironov D, Raschendorfer M, Reinhardt T, Ritter B, Schrodin R, Schulz JP, Vogel G. 2011. A description of the nonhydrostatic regional COSMO model, Part II: Physical Parameterization. Deutscher Wetterdienst, Offenbach, Germany, Available online at http://www.cosmo-model.org [Accessed on 20 May 2014], 161 pp.

Drobinski P, Ducrocq V, Alpert P, Anagnostou E, Béranger K, Borga M, Braud I, Chanzy A, Davolio S, Delrieu G, Estournel C, Filali Boubrahmi N, Font J, Grubisic V, Gualdi S, Homar V, Ivancan-Picek B, Kottmeier C, Kotroni V, Lagouvardos K, Lionello P, Llasat M, Ludwig W, Lutoff C, Mariotti A, Richard E, Romero R, Rotunno R, Roussot O, Ruin I, Somot S, Taupier-Letage I, Tintore J, Uijlenhoet R, Wernli H. 2014. HyMeX, a 10-year multidisciplinary program on the Mediterranean water cycle. *Bull. Amer. Meteor. Soc.* **95**: 1063–1082, doi:10.1175/BAMS-D-12-00242.1.

Drofa O, Malguzzi P. 2004. Parameterization of microphysical processes in a non hydrostatic prediction model. Proc. 14th Intern. Conf. on Clouds and Precipitation (ICCP), Bologna, 19-23 July 2004, 1297-1300.

Ducrocq V, Braud I, Davolio S, Ferretti R, Flamant C, Jansa A, Kalthoff N, Richard E, Taupier-Letage I, Ayral PA, Belamari S, Berne A, Borga M, Boudevillain B, Bock O, Boichard JL, Bouin MN, Bousquet O, Bouvier C, Chiggiato J, Cimini D, Corsmeier U, Coppola L, Cocquerez P, Defer E, Delanoë J, Girolamo PD, Doerenbecher A, Drobinski P, Dufournet Y, Fourrié N, Gourley JJ, Labatut L, Lambert D, Le Coz J, Marzano FS, Molinié G, Montani A, Nord G, Nuret M, Ramage K, Rison B, Roussot O, Said F, Schwarzenboeck A, Testor P, Baelen JV, Vincendon B, Aran M, Tamayo J. 2014. HyMeX-SOP1, the field campaign dedicated to heavy precipitation and flash flooding in the northwestern Mediterranean. *Bull. Amer. Meteor. Soc.* **95**: 1083–1100, doi:10.1175/BAMS-D-12-00244.1.

Ducrocq V, Nuissier O, Ricard D, Lebeaupin C, Anquetin S. 2008. A numerical study of three catastrophic precipitating events over southern France. II: Mesoscale triggering and stationarity factors. *Q. J. R. Meteorol. Soc.* **134**: 131–145.

Ferretti R, Pichelli E, Gentile S, Maiello I, Cimini D, Davolio S, Miglietta MM, Panegrossi G, Baldini L, Pasi F, Marzano FS, Zinzi A, Mariani S, Casaioli M, Bartolini G, Loglisci N, Montani A, Marsigli C, Manzato A, Pucillo A, Ferrario ME, Colaiuda V, Rotunno R. 2014. Overview of the first HyMeX Special Observation Period over Italy: observations and model results. *Hydrol. Earth Syst. Sci.* **18**: 1953–1977, doi:10.5194/hess-18-1953-2014.

Flamant C. 2013. Water vapour DiAL LEANDRE 2, ATR42/SAFIRE, version 2. *HyMeX database*, doi:10.6096//MISTRALS-HYMEX.WATER_VAPOUR DIAL LEANDRE2.V2.

Hanley KE, Plant RS, Stein THM, Hogan RJ, Nicol JC, Lean HW, Halliwell C, Clark RA. 2014. Mixing length controls on high resolution simulations of convective storms. *Q. J. R. Meteorol. Soc.* **141**: 272–284, doi:10.1002/qj.2356.

Jorgensen DP, Weckwerth TM. 2003. Forcing and organization of convective systems. In Radar and Atmospheric Science: A collection of essays in Honor of David Atlas, Wakimoto RM, Srivastava R (eds), American Meteorological Society, Boston, pp 75-103.

Kohler M, Kalthoff N, Kottmeier C. 2010. The impact of soil moisture modifications on CBL characteristics in West Africa: A case study from the AMMA campaign. *Q. J. R. Meteorol. Soc.* **136**: 442–455.

Manzato A. 2007. The 6 h climatology of thunderstorms and rainfalls in the Friuli Venezia Giulia Plain. *Atmos. Res.* **83**: 336–348.

Manzato A, Davolio S, Miglietta MM, Pucillo A, Setvak M. 2015. 12 September 2012: A supercell outbreak in NE Italy? *Atmos. Res.* **153**: 98–118, doi:10.1016/j.atmosres.2014.07.019.

Morcrette JJ, Barker HW, Cole JNS, Iacono MJ, Pincus R. 2008. Impact of a new radiation package, McRad, in the ECMWF Integrated Forecasting System. *Mon. Wea. Rev.* **136**: 4773–4798.

Nuissier O, Ducrocq V, Ricard D, Lebeaupin C, Anquetin S. 2008. A numerical study of three catastrophic precipitating events over southern France. I: Numerical framework and synoptic ingredients. *Q. J. R. Meteorol. Soc.* **134**: 111–130.

Rebora N, Molini L, Casella E, Comellas A, Fiori E, Pignone F, Siccardi F, Silvestro F, Tanelli S, Parodi A. 2013. Extreme rainfall in the Mediterranean: what can we learn from observations? *J. Hydrometeor.* **14**: 906–922.

Ricard D, Ducrocq V, Auger L. 2012. A climatology of the mesoscale environment associated with heavily precipitating events over northwestern Mediterranean area. *J. Appl. Meteor. Climatol.* **51**: 468–488.

Ritter B, Geleyn JF. 1992. A comprehensive radiation scheme for numerical weather prediction models with potential applications in climate simulations. *Mon. Wea. Rev.* **120**: 303–325.

Romero R, Doswell CA, Ramis C. 2000. Mesoscale numerical study of two cases of long-lived quasi-stationary convective systems over eastern Spain. *Mon. Wea. Rev.* **128**: 3731–3751.

Rotunno R, Houze RA. 2007. Lessons on orographic precipitation from the Mesoscale Alpine Programme. *Q. J. R. Meteorol. Soc.* **133**: 811–830.

Schättler U, Doms G, Schraff C. 2013. A description of the nonhydrostatic regional COSMO-model, Part VII: User's Guide. Deutscher Wetterdienst, Offenbach, Germany, Available online at http://www.cosmo-model.org [Accessed on 20 May 2014], 200 pp.

Tiedtke M. 1989. A comprehensive mass flux scheme for cumulus parameterization in large-scale models. *Mon. Wea. Rev.* **117**: 1779–1800.

Wicker LJ, Skamarock WC. 2002. Time-splitting methods for elastic models using forward time schemes. *Mon. Wea. Rev.* **130**: 2088–2097.